Accepted Manuscript

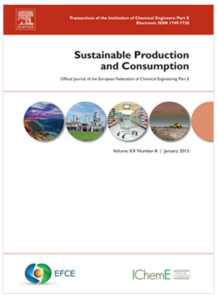

The carbon footprint of power-to-synthetic natural gas by photovoltaic solar powered electrochemical reduction of CO_2

Antonio Dominguez-Ramos, Angel Irabien

PII: S2352-5509(18)30211-2
DOI: https://doi.org/10.1016/j.spc.2018.11.004
Reference: SPC 186

To appear in: *Sustainable Production and Consumption*

Received date : 31 May 2018
Revised date : 30 October 2018
Accepted date : 5 November 2018

Please cite this article as:, The carbon footprint of power-to-synthetic natural gas by photovoltaic solar powered electrochemical reduction of CO_2. *Sustainable Production and Consumption* (2018), https://doi.org/10.1016/j.spc.2018.11.004

The carbon footprint of Power-to-Synthetic Natural Gas by Photovoltaic solar powered Electrochemical Reduction of CO_2

Antonio Dominguez-Ramos, Angel Irabien

Departamento de Ingenierías Química y Biomolecular, ETS Ingenieros Industriales y de Telecomunicación, Universidad de Cantabria, Avda. Los Castros s.n., Santander, 39005, Spain

Corresponding author: domingueza@unican.es, telephone: +34 94. 201474

Abstract

The search for more sustainable production and consumption patterns implies the integration of emerging edge-cutting technologies in the frontier research. However, holistic studies are needed in order to evaluate properly the environmental competitiveness of the suggested solutions. In this work, we use the Power-to-Gas approach to analyse the environmental rationality in terms of the carbon footprint (CF) of a Photovoltaic (PV) solar powered Electrochemical Reduction (ER) process for the utilisation of CO_2 as carbon source for the production of CH_4. This synthetic natural gas is ready to be injected into the transmission and distribution network. The raw materials for the process are a source of CO_2 (mixed with different ratios of N_2), H_2O and electricity from PV solar. The separated products are CH_4, C_2H_4, H_2/CO, O_2 and HCOOH. The reaction, separation/purification and compression stages needed to deliver commercial distributable products are included. Mass and energy balances were used to create a black-box model. The input to the model is the faradaic efficiency of best cathodes performing at lab-scale (over 60% faradaic efficiency towards CH_4) and its cathodic potential. Long-lasting cathodes were assumed. The output of the model is the distribution of products (related to 1 kg of pure CH_4) and the energy consumption at each of the mentioned stages. These energy consumptions are used to calculate the overall CF depending on the CF of the PV solar reference chosen.

The influence of the purity of the CO_2 stream used was analysed together with the conversion of the CO_2 in the reactor, showing the high contribution (over 60%) of the ER reaction stage even if diluted CO_2 is used. When a CO_2 conversion of 50% is chosen together with an inlet stream with a N_2:CO_2 ratio of 24, the electricity consumption of the process is between 2.6 and 6.2 times the minimum obtained for a reference ER

reactor including the separation and compression of gaseous products (18.5 kWh·kg^{-1} of CH_4). The use of PV solar energy with low CF ($14 \cdot 10^{-3}$ kg·kWh^{-1}) allows the current lab-scale performers to even the CF associated with the average world production of natural gas when the valorisation of C_2H_4 is included (~1.0 kg·kg^{-1} of CH_4).

Keywords

Electrochemical reduction; Power to gas; carbon footprint; PV solar energy; life cycle assessment;

Highlights

- The carbon footprint (CF) of a PV solar powered electro-reduction for CH_4 was analysed
- All relevant stages as reaction, separation of CO_2 and CH_4 and compression are included
- Between 2.6 and 6.2 times is the current electricity consumption compared to reference conditions
- The main contribution in CF terms is the reaction stage
- The CF of best performer can even the CF of the existing process for CH_4

1. Introduction

The 2030 Agenda for Sustainable Development is *"...a plan of action for people, planet and prosperity"* (United Nations, 2015). This global agenda includes a set of 17 Sustainable Development Goals, with the purpose of guiding international/national/local development policy actions towards the fulfilment of those goals and their individual corresponding 169 targets in 2030. Energy, as a basic element of human prosperity, and its environmental consequences are featured in several goals. 7 ("ensure access to affordable, reliable, sustainable and modern energy for all"), 12 ("ensure sustainable consumption and production patterns"), and 13 ("take urgent action to combat climate change and its impacts"). To reach such global goals highlighting the intimate relationship of energy and Climate Change, and, in parallel with the on-going massive integration of renewable sources in the power sector, a form of storing energy is necessary due to the intermittent and stochastic behaviour of wind and solar irradiation.

Electricity, as a form of energy, can be directly stored as electrical charges and indirectly as kinetic, potential or chemical/electrochemical energy (Dunn et al., 2011; Liu et al., 2010; Yang et al., 2011). In this work, the focus is upon the potential interactions as an energy storage between the electrical grid or power network (electricity) and the natural gas (NG) pipeline network (heating services/commodity/transportation) through the well-known Power-to-Gas technologies, which has gathered a noticeable interest recently (Bailera et al., 2017; Götz et al., 2016; Mazza et al., 2015).

The European Power-to-Gas Platform defines Power-to-Gas (PtG) as "*the functional description of the conversion of electrical power into a gaseous energy carrier like e.g. hydrogen or methane*" (European Power to Gas Platform, 2018). Hereafter, as the target product in this study is CH_4, it will be used preferentially the title of Power-to-Synthetic Natural Gas (PtSNG). Thanks to the PtSNG, the excess of intermittent renewable sources can be stored as CH_4 without using the mediation of electrolytically produced H_2 as energy carrier for the methanation of CO_2. In this sense, the current adopted approach seems to rely on the participation of H_2 as intermediate to produce the CH_4 by methanation (Schiebahn et al., 2015).

Carbon Capture and Use (CCU) of CO_2 can be understood as the transformation of CO_2 into valuable chemicals or fuels, trying to widen the portfolio of technologies at the gigatonne scale (Majumdar and Deutch, 2018). There is a myriad of technological

options to proceed with a transformation from such a very stable molecule (Appel et al., 2013; Dimitriou et al., 2015; Kondratenko et al., 2013). Among all potential routes, we do propose here the Electrochemical Reduction (ER) of CO_2, a technology that has received a lot of attention in the past decade (Jhong et al., 2013; Kenis et al., 2017; Whipple and Kenis, 2010; Zhang et al., 2018). Thanks to this technology, CO_2 has been successfully reduced at lab-scale to other forms such as CH_3OH (Albo et al., 2017, 2015; Goeppert et al., 2014; Lee et al., 2016; Merino-Garcia et al., 2017; Olah et al., 2009; Sebastián et al., 2017; Zhao et al., 2017), CO (Hernández et al., 2017; Kas et al., 2016; Khezri et al., 2017; Rosen et al., 2011; Ross et al., 2017), HCOOH (Alvarez-Guerra et al., 2014; Del Castillo et al., 2015, 2017; Gao et al., 2016; Kopljar et al., 2016; Lee and Kanan, 2015; Li and Oloman, 2005; Min and Kanan, 2015; Natsui et al., 2018; Oloman and Li, 2008; Scialdone et al., 2016; Yang et al., 2017; S. Zhang et al., 2014; Zhu et al., 2016), and of course, CH_4 (Cook, 1989; DeWulf et al., 1989; Hori et al., 2002, 1986; Kaneco et al., 2006; Manthiram et al., 2014; Merino-Garcia et al., 2018, 2017, 2016; Varela et al., 2016; Weng et al., 2018) thanks to an applied voltage when proper well-tuned catalytic electrodes are used (Qiao et al., 2014). The ER process will then demand the mentioned CO_2 as C source; a "cheap" source of protons, mainly from water; and renewable electricity for the power demanded by the entire process, in which the electrochemical reactor can play a major role. The reference renewable source of choice in this work is Photovoltaic (PV) solar energy due to the expected main contribution to global energy demand (Breyer et al., 2017), making this technology the only one on track of its International Energy Agency Sustainable Development Scenario (International Energy Agency, 2018).

Of course, the ER of CO_2 is not free of disadvantages. Three key issues must be highlighted here. The first issue is the fact that the reduction does not provide a pure targeted product but a mixture of them (Greenblatt et al., 2018) due to the existence of parasitic parallel reactions. Consequently, additional energy penalties are encountered. The second is the fact that the cathode lifetime is still a technical circumstance as the desired efficiency only last in the range of hours under current developments (Martin et al., 2015). Thirdly, the reduction process is evidently a huge energy consumer, as the oxidation reaction must be turned back to a reduced carbon state.

Figure 1 presents the framework of the present study. The CO_2 from point sources such as the power sector or any other industrial process can be returned to the production of SNG and other products from ER such as C_2H_4, being powered by the

excess of PV solar energy that is not accepted in the power network. In turn, this SNG can used in the power sector adding extra flexibility to the operation of both networks. This is the reason behind SNG must not be conceived as a fossil fuel but as a renewable fuel as the source for its production is based on renewable sources such as PV solar. Saving of natural resources such as NG is possible as SNG is injected in the NG network, partially avoiding the extraction of NG from wells. Therefore, we do coin here the term artificial CO_2 sink due to the production of SNG instead of the direct release of CO_2 to the atmosphere. To be a true artificial sink, the connection of the ER to renewable low carbon sources of electricity such as PV solar is necessary. The only CO_2 losses comes from the use of the NG at places in which the conversion is not possible (homes, buildings, automobile, small factories, etc.). The followed approach is in line with similar views for the CCU in which the connection to renewable sources is essential (Abanades et al., 2017) or the production of more than one single product is considered (Fernández-Dacosta et al., 2018).

The carbon footprint of the SNG production CF_{CH_4} will be determined by two terms: i) the energy consumption of the different individual process stages, and ii) its corresponding carbon footprint. The renewable energy sources has its own carbon footprint derived from the required infrastructure. The threshold for the acceptable carbon footprint of those renewable sources of electricity is described in this work. The benchmark for the comparison is the average world distribution of NG, which is also depicted in Figure 1. The possibility to "electrify" a chemical process is a competitive advantage versus other thermochemical based approaches (Schiffer and Manthiram, 2017). All the emissions of CO_2 from the chosen source are avoided due to the *in-situ* transformation, thus, there is a strong argument to be considered as a mitigation alternative.

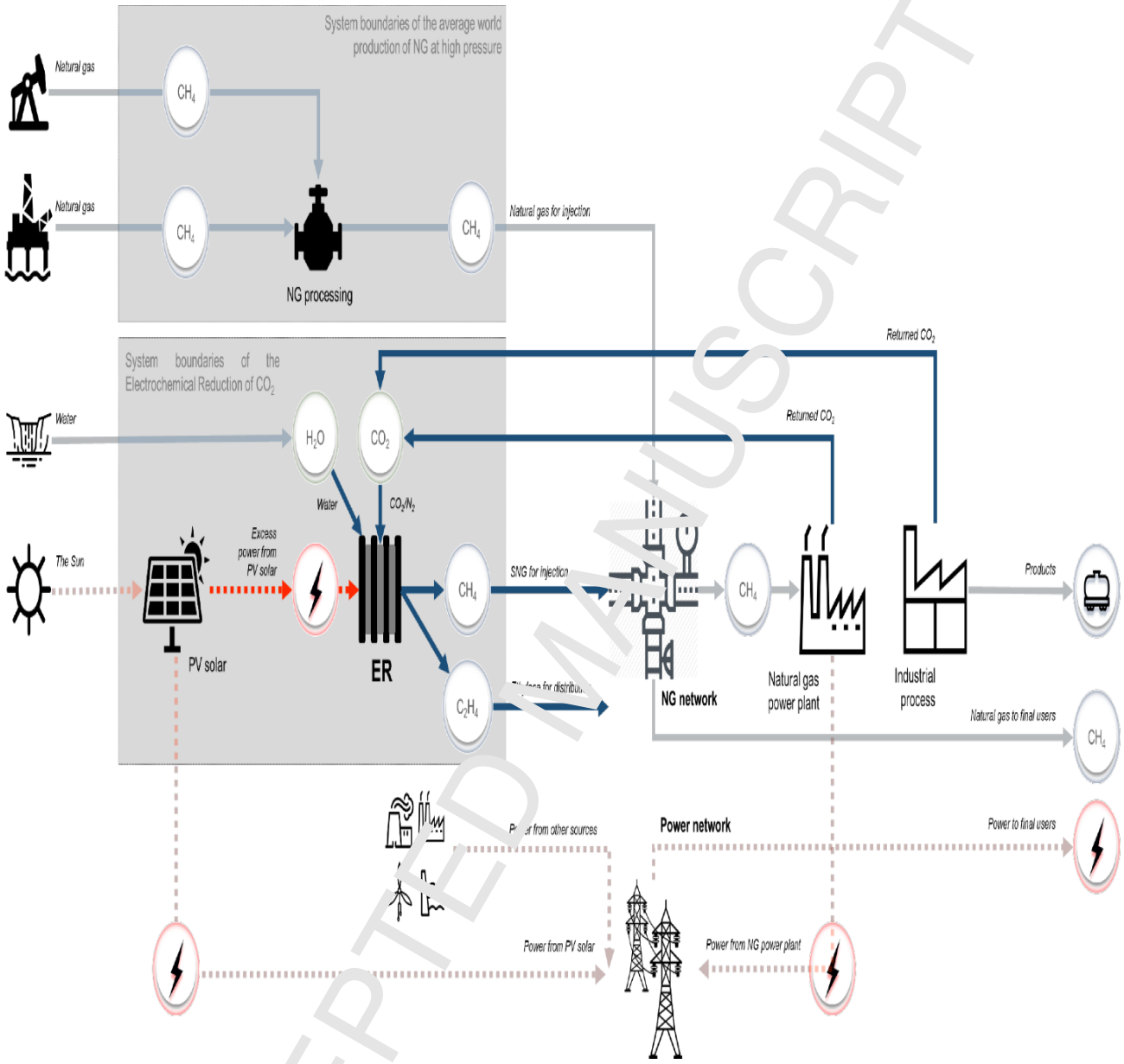

Figure 1. Framework of the Power-to-Synthetic Natural Gas (PtSNG) by means of Electrochemical Reduction (ER) of CO_2 from point sources using PV solar.

156

Undoubtedly, the quantification of the carbon footprint of any technology strongly relies on the Life Cycle Assessment (LCA) tool, in order to guarantee that every single involved process is accounted for (Finnveden et al., 2009), even more in the case of CCU (Cuéllar-Franca and Azapagic, 2015). The impact category of choice is Global Warming, which has been already referred in this work as carbon footprint (CF). The utilization of CO_2 by the PV solar powered ER from any point CO_2 source does not mean that the CO_2 is removed from the atmosphere, which is a relevant flaw (von der Assen et al., 2013), but the fate of that CO_2 determines its actual contribution to Global Warming. A detailed review of the application of LCA for the conversion of CO_2 by different catalytic routes can be found in the literature (Artz et al., 2018). Specific literature regarding the application of LCA to PtG can be also identified recently (Collet et al., 2017; Parra et al., 2017; Reiter and Lindorfer, 2015; Sternberg and Bardow, 2016; Zhang et al., 2017).

To understand the goal and scope of this work, a simple but effective rationality of using renewables sources of electricity for the PtSNG by ER is given next. The reference theoretical production (no overpotential, 100% Faradaic Efficiency (FE), water oxidation at the anode) of CH_4 by ER requires a minimum specific energy consumption of SEC_{CH_4} of 14.2 kWh·kg^{-1} of CH_4. The PV solar energy has a carbon footprint (CF_{PV}) which belongs to the range between a low value CF_{PV-L} of $14 \cdot 10^{-3}$ kg CO_2-eq.·kWh^{-1} and a high vale CF_{PV-H} of $58 \cdot 10^{-3}$ kg CO_2-eq.·kWh^{-1} for the year 2010 (Hertwich et al., 2015). Consequently, the reference production of CH_4 means that the use of the PV solar powered ER would lead eventually to a net release of 0.2 kg CO_2-eq.·kg^{-1} of CH_4 if the low value is considered. This value is below the carbon footprint of the actual world average natural gas distribution CF_{Eco-NG} at 0.46 kg CO_2-eq.·kg^{-1} of CH_4 (Ecoinvent, 2017), which account for CH_4 losses and CO_2 emissions along the transmission and distribution network. Missing the current technical developments therefore can help at elucidating wrong conclusions. Indeed, the CF_{PV} is expected to be ultra-low by 2050 ($5 \cdot 10^{-3}$ kg CO_2-eq.·kWh^{-1}) as stated in (Pehl et al., 2017), which in turn will make the PV solar powered ER to provide CH_4 with a value as low as 0.071 kg CO_2-eq.·kg^{-1} of CH_4. It is the ER the technology that get benefits of the developments in the clean power field.

188 Table 1. Comparison of techno-environmental-economic studies of the electrochemical reduction of CO_2 to different products. Topic related
189 studies for the capture of CO_2 are also included for reference purposes. ER stands for Electrochemical Reduction, SEP for Separation, FT for
190 Fischer-Tropsch, *FE* for Faradaic Efficiency, PV for Photovoltaic, MEA for Monoethanolamine, DAC for Direct Air Capture, PSA for Pressure
191 Swing Adsorption.
192

	Sustainability pillars		Stages					Approaches	
	Environmental	Economic	Target ER products	ER	SEP of CO_2	SEP of ER products	Distribution of gaseous ER products	Life Cycle	Integration of renewables
This work	Carbon Footprint	No	CH_4, C_2H_4, H_2, HCOOH (cathode) and O_2 (anode).	Analysis of cell voltage and FE (up to 10 references with different FE and cathode potentials	Unconverted CO_2 in the ER reactor	Based on the approach given by (House et al., 2011). Including distillation of HCOOH/water distillation	Compression of gaseous products	Updated Carbon footprint of the electricity used and integration of all stages to provide a commercial product	PV solar energy for the electricity consumption
(Li et al., 2016)	Carbon Footprint	Levelized cost of the fuel	CO (for later diesel production from FT processing + external	Analysis of the effect of FE, current density and cell voltage	Unconverted CO_2 in the ER reactor by PSA	No needed		Well-to-gate CO_2	High performance scenario (zero emissions from the

			electrolyzed H_2)						generated electricity)
(Verma et al., 2016)		Gross-margin model of ER products	HCOOH, CO, CH_3OH, CH_4, C_2H_4, C_2H_5OH	Analysis of the effect of cell voltage, FE, and current density		Based on Sherwood plot (for cost calculations)			
(Jouny et al., 2018)	Brief mention to carbon footprint	Net Present Value of ER products	$CH_3CH_2CH_2OH$, HCOOH, CO, C_2H_4, C_2H_5OH, C_2H_4, CH_3OH	Product selectivity, cell voltage and current density (base and optimistic case)	CO_2 capture and purification (by MEA or DAC) Unconverted CO_2 in the ER reactor (by PSA)	Distillation for $HCOOH/H_2O$ mixtures	Neglected		Brief mention to PV solar and wind energy for the electricity consumption
(Greenblatt et al., 2018)	Energy demand	No	CO, HCOOH, $CH_3CH_2CH_2OH$, CH_4, C_2H_4, C_2H_5OH, $CH_3CH_2CH_2OH$, C_{4+} HC	No	CO_2 source for the ER	A detailed and vast list of options is included along with the energy requirements		Embodied energy of the solvents and polymers (membrane) used	Photo electro chemical integrated system
(Agarwal et al., 2011)		Net Present Value	HCOOH/HCOO$^-$	Electricity consumption, catalysis lifetime and	Not mentioned	Not mentioned		Value-chain	Brief mention to PV solar and wind

				electrolyte consumption					energy for the electricity consumption
(Chen and Lin, 2018)	Carbon Footprint	No	All conventional ER products	Electricity consumption based on the cell current efficiency and peripheral sources (electrolytes, auxiliary operations and infrastructure)	No	Not included		CO_2 contribution of peripheral sources (electrolytes, auxiliary operations and infrastructure)	The use of fossil fuel power is justified
(Spurgeon and Kumar, 2018)		Cost of produced fuel	HCOOH, C_2H_5OH, and $C_{2+}HC$ by FT processing (through CO)	Analysis of the effect of FE, current density and cell voltage	CO_2 capture and purification (by MEA) Unconverted CO_2 in the ER reactor (by PSA)	Not included			Brief mention to PV solar and wind energy for the electricity consumption

193

Thereupon several studies have been published regarding the techno-environmental-economic feasibility of the ER to several products. Table 1 aims at the comparison of the main issues in order to identify existing gaps of the previous approaches. As it can be seen in Table 1, studies were limited at some point on their scopes regarding the impact of the electricity source, the CO_2 source and the integrated individual stages requested for the manufacture of commercial products from an ER process (reaction and separation/purification). The novelty of this work relies this on the simultaneous consideration of all the relevant individual stages coupled to an ER process (upstream processing, reaction and downstream processing) considering the top performance lab-scale data of updated references for the PtSNG by PV solar powered ER of CO_2 under a life cycle approach. The economic assessment is out of the scope of this work. The readers are referred to the papers in Table 1 for additional information on techno-economic studies.

Therefore, the goal of this work is to analyze the environmental rationality in terms of Carbon Footprint (CF) behind using low carbon electricity sources such as Photovoltaic solar (PV) for a Power-to-Synthetic Natural Gas (PtSNG) process based on the Electrochemical Reduction (ER) of CO_2. This vision leads to the saving of a natural resource such as natural gas (NG). This way, NG is not extracted from nature anymore. Simultaneously, there is a net reduction of emissions of CO_2 due to its use as raw material from the very source due to the utilization of technology that allows the electrification of the overall process. The scope of this work considers a PtSNG process in which the influence of the upstream processing (purity of the CO_2 source and CO_2 conversion), the reaction stage (faradaic efficiency and cathode potential) and the downstream processing (separation of unreacted CO_2 and diluting N_2, separation/purification of ER products and compression to commercial distributable conditions) is discussed. The best performance lab-scale data with a Faradaic Efficiency (FE_{CH_4}) over 90% to CH_4 is used as basis for the ER stage. Mass and energy balances are applied to each individual stage. The reference used is the production of 1 kg of pure CH_4 ready for injection in the NG network.

2. Methodology

The CF_{CH_4} of the PV Solar powered ER to CH_4 requires first the definition of the boundaries of the process. Figure 2 shows the process flow diagram chosen in this study. The core of the process is the ER reactor. Additional stages for the separation of gas and liquid products as well as for gas compression are also added. Output gaseous products are high-purity CH_4, C_2H_4, H_2 (combined with CO as syngas when corresponding) and liquid 85% wt. HCOOH (in water) from the catholyte. Gaseous O_2 is produced in the anolyte. Sources with different CO_2 purity (due to the presence of N_2) are considered. Water is used as a source of protons. Thus, the inlet streams are CO_2/N_2 mixtures and water. The influence of the purity of the CO_2 used as raw material under different conversions in the reactor (upstream processing) and the effect of the faradaic efficiencies and cathode voltage U_C obtained in current top performer electrodes at lab-scale (reaction) are covered within this study. Separation and compression of the obtained gaseous products as well as purification of the liquid product (downstream processing) is also included.

Regarding the modelling of the process, steady state conditions are assumed. To check the validity of results, mass balances were completed for the i products (CH_4, C_2H_4, H_2/ CO, HCOOH and O_2), thus inputs are balanced with the outputs for the j existing streams. Individual k stages are modelled as black-boxes. The input data is reported in Table 2 as the set of faradaic efficiencies of the i^R reduction products (CH_4, C_2H_4, H_2, CO, HCOOH) FE_{iR} for the considered studies of reference as top performers at lab-scale. Additionally, a set of different parameters (e.g. temperature of reference T_{REF}) and process conditions (such as the CO_2 conversion per pass X_{CO_2}) are also used as input data. The output data from the model is the amount of mass of each i product m_i and the energy consumption in each k stage EC_k: reaction, separation of CO_2/N_2, separation of CH_4 and the other gaseous products, compression (as electricity), and distillation (as heat) per unit of mass of CH_4. The mixing stage prior to the reaction and the gas/liquid separator have no energy consumption. The output data of the model (m_i and EC_k) is used in combination with reported carbon footprint data of the PV solar energy (CI_{PV}) to transform the required amount of electricity/heat into the overall carbon footprint CF_{CH_4} measured as mass of CO_2-eq. per unit of mass of CH_4 ($kg \cdot kg^{-1}$). The carbon footprint associated to the infrastructure required for the process is

neglected due to the low stability of the electrodes, which is true not only for the production of CH_4 but for other ER products (Martin et al., 2015). Otherwise, the CF_{CH_4} would be so high that it will dwarf the contribution of the different processing stages. Long-lasting cathodes are considered here.

2.1 Upstream processing: Purity of the CO_2 source

In order to take into account the potential effects of the purity of the CO_2 source over the entire process, different molar ratios CO_2/N_2 as feed to the ER were used. The values of the molar fractions of the CO_2/N_2 mixtures used here are representative from different industry sectors (Bains et al., 2017), trying to cover the full range of CO_2 concentrations.

2.2 Reaction: Electrochemical reactor operating conditions for top performers at lab-scale

The ER reactor, which industrially would be conceived as a set of cell stacks, is assumed here as a divided cell (two separated compartments). In the catholyte, the ER of CO_2 delivers several i^R reduction products in a gaseous form: CH_4, C_2H_4, H_2, CO and one a liquid form, HCOOH. In the anolyte, the only i^O oxidation product is gaseous O_2. The product distribution in the cathode depends on the faradaic efficiency for each i^R product FE_{i^R}. Due to be independent compartments, the catholyte is conducted to a gas/liquid separator; this way, the liquid phase is subjected to an additional distillation process and the gas phase to further processing. The first downstream processing consist on the separation of the CO_2 and the N_2 from the other gaseous products of the reactor. The CO_2 that reaches that separation unit is the unconverted CO_2 from the ER reactor, while N_2 comes from the CO_2 source (it is assumed that it does not participate in the reaction). As hypothesis, wherever the molar fraction of N_2 is, there is no influence on the kinetics on the process, thus the direct consequence is an additional separation energy cost in the corresponding separation stage.

Table 2 summarizes the current top lab-scale performance for the ER of CO_2 to CH_4 under the experimental conditions that provides the maximum FE_{CH_4} value. Selected references display FE_{CH_4} over 60%. In this work, it is hypothesized that the lifetime of the electrode or its performance remains stable for a set of hours large enough, thus its carbon footprint can be neglected. Some of the references used in this work here did not

stated explicitly the stability of the electrode, but it can elucidated that they typically last less than 2 hours. This short electrode stability is coherent compared to other values previously reported even for other ER products (Martin et al., 2015). Indeed, progress is on-going as available CO_2 electrolysers report voltage increases as low as ~$6 \cdot 10^{-6}$ V·h^{-1} (Dioxide Materials, 2018). Working with the chosen electrodes is only possible under the hypothesis of long-lasting electrodes. The chosen metal for the ER of CO_2 to CH_4 is Cu, with a clear temporal trend from foil sheets to nanoparticles. Theoretical calculations on the higher yields of CH_4 and C_2H_4 yields on Cu over CH_3OH were recently proposed (Hussain et al., 2018). The current density CD values are moderate, ranging from 5 mA·cm^{-2} to 22.7 mA·cm^{-2}. On the other hand, the cathode potential U_C ranged from -3.8 V vs NHE to -1.35 V vs NHE, still far away from the theoretical minimum cathode voltage of 0.169 V vs NHE (Ganesh, 2016). Typical electrolyte for the reduction is $KHCO_3$ in concentrations ~0.1 mol·L^{-1}. In order to reduce the complexity of the separation process, it is assumed that electrolytes can be perfectly recirculated. The effect in the ER process of the electrolyte consumption is studied from an economic point of view in (Agarwal et al., 2011). When data is not presented for the all the i^R species, a round up was used to present a 100% faradaic efficiency as summation of the FE_{i^R} of each of the five i^R products (Pander III et al., 2017). If the FE_{i^R} for a i^R product is not stated explicitly, 1% FE_{i^R} is assumed as a default value. The FE_{CO} is relatively low, with the exception of 15% from (Kaneco et al., 1999). For this particular reference, it is evident that syngas (H_2/CO) is produced instead of H_2 as pure product. H_2 and CO are considered as individual product for the sake of calculations but they are not separated in the later stages.

The conversion of CO_2 per pass through the ER reactor X_{CO_2} is assumed to be established at 50% (Jouny et al., 2018). When the influence of X_{CO_2} is studied, the lower range reported by (Jouny et al., 2018) of 10% is considered. We did assume a maximum conversion of 99%. Other potential conversion values of 25%, 50% and 75% were mentioned in (Spurgeon and Kumar, 2018). Because of the recirculation, all the CO_2 at the source is consumed within the boundaries of the process, thus no CO_2 is finally released.

One of the key elements of the process is the assessment of the Specific Energy Consumption of each i^R reduction product SEC_{ER-i^R} (kWh·kg^{-1}), which is defined as follows in Eq. 1:

$$SEC_{ER-i^R} = \frac{n_{i^R} F |U_C - U_A|}{3600 \cdot MW_{i^R} \cdot \left(\frac{FE_{i^R}}{100}\right)} \quad \text{Eq. 1}$$

where n_{i^R} is the number of moles of electrons involved in the reaction (8 for CH_4, 12 for C_2H_4, 2 for H_2, 2 for CO, and 2 for HCOOH); F is the Faraday constant (96,485 C·mol^{-1} electrons); U_C is the cathode potential (V vs NHE); U_A is the anode potential (V vs NHE); and MW_{i^R} is the molecular weight of the i^R product (g·mol^{-1}). The cathode potential values U_C are reported in Table 2 for each selected reference. The values for U_A are derived from the minimum theoretical potential for the oxidation of water at 1.23 V vs NHE (at a pH value of 0) plus a typical reference overpotential at 0.5 V (Jouny et al., 2018; Kauffman et al., 2015). Assuming the use of high concentrated KOH solution in the anolyte compartment, a very high pH around 14 can be used thus -0.0592 V were subtracted per unit of pH, rendering a total value of U_A at 0.90 V. Additional potential losses from electrolytic compartments and separation membranes are neglected. Further work is envisaged to quantify this contribution, so the total cell potential is below the maximum expected real value.

The overall basis for the calculation is 1 kg of CH_4, thus EC_{ER-CH_4} is the energy consumption used in the ER reaction stage. In order to quantify the relative production of the reduction products m_i, the total amount of electricity for the production of CH_4 is used, along with its SEC_{ER} according to Eq. 2:

$$\frac{SEC_{ER-i^R}}{SEC_{ER-CH_4}} = \frac{m_{CH_4}}{m_{i^R}} \quad \text{Eq. 2}$$

The stoichiometric amounts of CO_2 and H_2O are included as inputs in the process. Consumption of CO_2 takes place in the cathode for the different reduction reactions. Consumption of H_2O does in the anode for the oxygen evolution reaction. The H_2O used for the liquid phase of the catholyte is also included (derived from using a liquid phase for the reduction).

2.3 Downstream processing

2.3.1 Gas and liquid streams separations

The catholyte from the ER reactor has two phases. The liquid phase corresponds to the HCOOH formed alongside with the H_2O that forms the catholyte. We used a ratio of 10 moles of water per mole of HCOOH, as it is not possible to obtain a better figure from current references due to the low homogeneity of the experimental set-up. The k^T thermal energy consumption for the distillation process of the azeotropic H_2O-HCOOH mixture EC_{DIST} (kJ) needed for the purification of HCOOH up to the commercial purity of 85% wt. was obtained in a previous work (Dominguez-Ramos et al., 2015). The amount of H_2O could be potentially headed back to the ER reactor. If heat (as steam) is industrially sourced from natural gas, the corresponding carbon footprint of the used heat CF_{Heat} is $123 \cdot 10^{-6}$ kg·kJ^{-1}, which is derived from (Ecoinvent, 2017).

A pure stream of O_2 is obtained at the anode of the reactor. The separation of the i^R products from the gaseous stream from the cathode results into three streams. One of those streams is the unconverted CO_2, which is mixed back prior to entering the ER reactor. The second stream is the one containing N_2, which is accompanied by the residual amount of O_2 from the reduction to CO, which is purge out of the system. The third stream includes all the valuable products. The separation of these three gaseous products takes place in a similar separation process, which includes CH_4, C_2H_4, H_2/CO (in a ratio that depends on each reference). Expected purities of the products are summarised in Table 1 of the SI (syngas is modelled as pure H_2). It is assumed that the energy consumption for the k^{NT} non thermal separation process (SEP-CO_2 and SEP-CH_4) regarding the i^R reduction gaseous product $EC_{k^{NT}}$ (kJ) are based on the minimum thermodynamic energy consumption based on the mixing entropy according to Eq. 3:

$$EC_{k^{NT}} = \frac{100}{f_{k^{NT}}} \left[-RT_{REF} \sum_{j^{k^{NT}}} v_{j^{k^{NT}}} \left[n_{j^{k^{NT}}} \sum_{i^{k^{NT}}} x_{i^{k^{NT}} j^{k^{NT}}} Ln\left(x_{i^{k^{NT}} j^{k^{NT}}} \right) \right] \right] \quad \text{Eq. 3}$$

Where R is ideal gas constant ($8.314 \cdot 10^{-3}$ kJ·mol^{-1}·K^{-1}); T_{REF} is the reference temperature (298.15 K); $v_{j^{k^{NT}}}$ indicates whether the stream is an input (+1) or output (-1); $n_{j^{k^{NT}}}$ is the total molar amount of the $j^{k^{NT}}$ streams associated with the k^{NT} non thermal separation process; and $x_{i^{k^{NT}} j^{k^{NT}}}$ is the molar fraction of the $i^{k^{NT}}$ product in

the $j^{k^{NT}}$ stream. Molar fractions are used instead of fugacity coefficients due to the ideal assumed behaviour (Y. Zhang et al., 2014). $f_{k^{NT}}$ is a correction factor to transform the ideal minimum thermodynamic values into real-world energy consumption. For the energy separation of the CO_2/N_2 mixture EC_{SEP-CO_2}, a f_{SEP-CO_2} value of 15 was used. In turn, for the energy separation of the $CH_4/C_2H_4/H_2/CO$ mixture EC_{SEP-CH_4}, a more conservative value for the separation f_{SEP-CH_4} equal to 5 was used. These two $f_{k^{NT}}$ values were adopted from the work from (House et al., 2011) for similar separations. No enthalpy of mixing was added (Greenblatt et al., 2018).

2.3.2 Compression of gaseous products

In order to distribute a commercial product, a final stage of compression is needed for all the obtained gaseous i^G products (the purified CH_4, C_2H_4, H_2/CO plus the O_2). Table 1 of the SI provides the conditions for pressure and temperature conditions and its corresponding phase. A set of own simulations in Aspen Plus (Aspen Tech, 2018) were used to estimate the specific energy consumption for the compression of the gaseous products $SEC_{COMP}^{i^G}$ (kWh·kg^{-1}). For O_2, the $SEC_{COMP}^{O_2}$ value from (Singla and Chowdhury, 2017) was used instead. The values provided are in the order of magnitude of similar references. As it can be seen in Table 1 of the SI, different pressures and temperature conditions lead to different phases. The main targeted product here (CH_4) was compressed up to 97 bar to be directly injected in the natural gas network thus density can reach a value of 71 kg·m^{-3}. Procedures or combination for the simultaneous injection of CH_4/H_2 mixtures are out of the scope of this work.

2.4 Calculation of the carbon footprint

The calculation of the carbon footprint derived from the production of 1 kg of CH_4 plus the additional products CF_{CH_4} (expressed as kg of CO_2-equivalent per kg of CH_4) is quantified as follows in Eq. 4:

$$CF_{CH_4} = CF_{PV}\left[\sum_{k^E} EC_{k^E}\right] + CF_{Heat}\left[EC_{DIST}\right] \quad \text{Eq. 4}$$

Where k^E is the set of the k stages supplied by electricity (ER-CH_4, SEP-CO_2, SEP-CH_4 and COMP). Consequently, different CF_{PV} for the PV solar energy will provide

412 different values for the CF_{CH_4}. In case the contribution of EC_{DIST} is disregarded, the
413 second term in the previous summation is simply neglected. The output of the model
414 provides the values for EC_{ER-CH_4}, EC_{SEP-CO_2}, EC_{SEP-CH_4}, EC_{COMP} and EC_{DIST}.

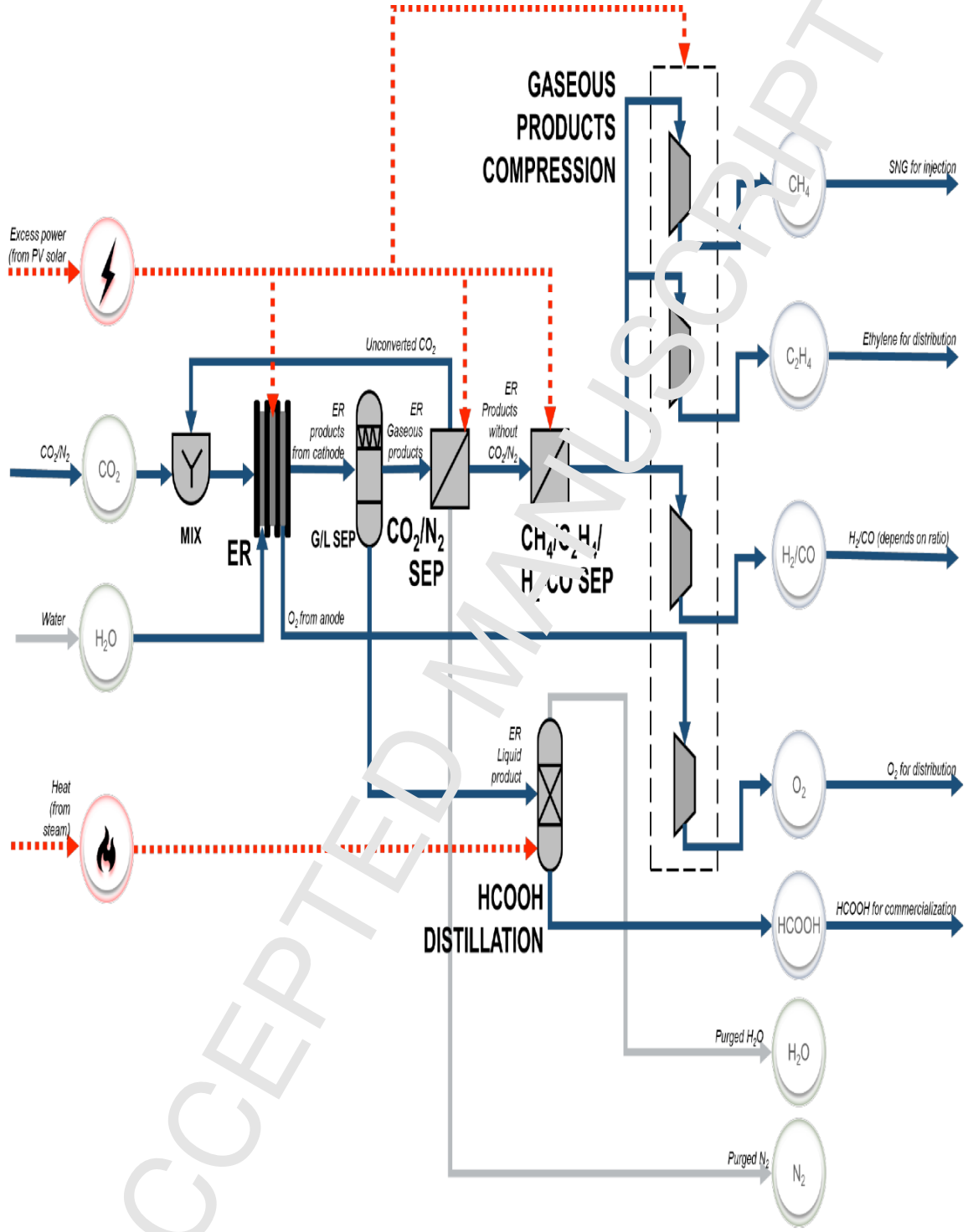

Figure 2. Process flowsheet diagram for the PV solar powered Electrochemical Reduction of CO_2 to Synthetic Natural Gas (PtSNG).

Table 2. Selection of top lab-scale performers for the ER of CO_2 to CH_4 ordered according to the reported best value for FE_{CH_4}. For a more detailed description of products obtained, duration of electrodes and their preparation, the reader is referred to the original references.

Reference	Type of copper used as cathode	CD	Catholyte		U_C	$FE_{i,R}$				
		$mA \cdot cm^{-2}$	$mol \cdot L^{-1}$	Substance	V vs. NHE	CH_4	C_2H_4	H_2	CO	HCOOH
(Manthiram et al., 2014)	Nanoparticles, supported on glassy carbon	12.5	0.1	$NaHCO_3$	-1.35	76	1[a]	21[b]	1[a]	1[a]
(Cook, 1988)	In situ uniformly deposited on glassy carbon	8.3	0.5	$KHCO_3$[d]	-1.7	73	25	1[a]	1[a]	0[c]
(Kaneco et al., 2006)	Foil	22.7	0.25	$NaClO_4$, in CH_3OH	-2.8	70.5	3.1	17.9	3.2	5.3[c] (4.2)[e]
(Varela et al., 2016)	Polycrystalline	14	0.2	$KHCO_3$	-1.43[b]	70[b]	15[b]	10[b]	1[b]	4[c]
(Weng et al., 2018)	Cu(II) phthalocyanine	20.5	0.5	$KHCO_3$	-1.06	66	2.5[b]	28[b,c]	1[b]	2.5[b]
(Hori et al., 1986)	Sheet	5	0.5	$KHCO_3$	-1.36	65	5[b]	20[b]	1[b]	9[c]
(Hori et al., 2002)	Single crystal Cu(S) (210)	5	0.1	$KHCO_3$	-1.52	60.5	11.6	7.3	2.6	18.0[c] (8.2)[e]
(DeWulf et al., 1989)	Foil	15	0.5	$KHCO_3$	-1.76	60	5	33[c]	1[a]	1[a]
(Kaneco et al., 1999)	Foil	12[a]	0.08	LiOH, in CH_3OH	-3.8	60	18	2[c]	15[b]	5[b]
(Baturina et al., 2014)	Electrodeposited	-	0.1	$KHCO_3$	-2.0	60[b]	19[b]	7.5[c]	5[c]	8.5[c]

[a] Not mentioned in the work, thus assumed as 1%; [b] Value estimated from graphs; [c] Includes the remaining FE; [d] $0.5 \cdot 10^{-4}$ M $CuSO_4$ (for electrodeposition); [e] in parenthesis the reported data for exclusively HCOOH

3. Results

3.1 Influence of the purity of the CO_2 source (upstream processing) and the conversion

To analyse the effect of the purity of the CO_2 stream, several conversions of CO_2 per pass through the ER reactor X_{CO_2} were studied, namely 10%, 50% and 99%. To remove the effect of the separation of the $i^{k^{NT}}$ products, a reference ER reactor with FE_{CH_4} of 100% was considered (at a pH value of 0). This way, a single effect is analysed. It is assumed that the dilution of the CO_2 has not an effect on the other experimental conditions (a detailed model of the ER reactor has not been used in this work). Figure 3 represents the energy contribution of the individual stages EC_{ER-CH_4}, EC_{SEP-CO_2}, and EC_{COMP} stacked up to 100%. The total energy consumption per unit of mass of CH_4 EC_{CH_4} (kWh·kg^{-1} CH_4) is also represented. As a reference ER reactor is considered here, EC_{SEP-CH_4} and EC_{DIST} are necessary zero.

As it can be seen in Figure 3a) for a X_{CO_2} of 10%, the contribution of EC_{ER-CH_4} can vary from 62% (4% molar in CO_2) to 83% (99% molar in CO_2), while the contribution of EC_{SEP-CO_2} does from 30% (4% molar in CO_2) to 6% (99% molar in CO_2). The contribution of EC_{COMP} ranges from 8% to 11%. On the other hand, for a X_{CO_2} of 99% as it is shown in Figure 3c) for the most concentrated stream, the contribution of EC_{ER-CH_4} can be as high as 88%, being the other significant contributor the EC_{COMP} with the remaining 12%. In this case, the EC_{CH_4} can be as low as 16.1 kWh·kg^{-1} CH_4. For the X_{CO_2} of 50%, intermediate values are evidently obtained as it is displayed in Figure 3b). It is clear that an extended conversion leads to lower energy consumption of the separation of the unreacted CO_2. ER reactor design should be also focused in the effort to develop the maximum possible conversion to reduce in turn as much as possible the energy consumption derived from the separation. For the lower conversion X_{CO_2} of 10%, the most diluted source of CO_2, which is the post combustion gases from burning natural gas (4% molar in CO_2), means that EC_{ER-CH_4} contributes only 62%. The remaining separation and compression stages represents the remaining 38% of the electricity consumption.

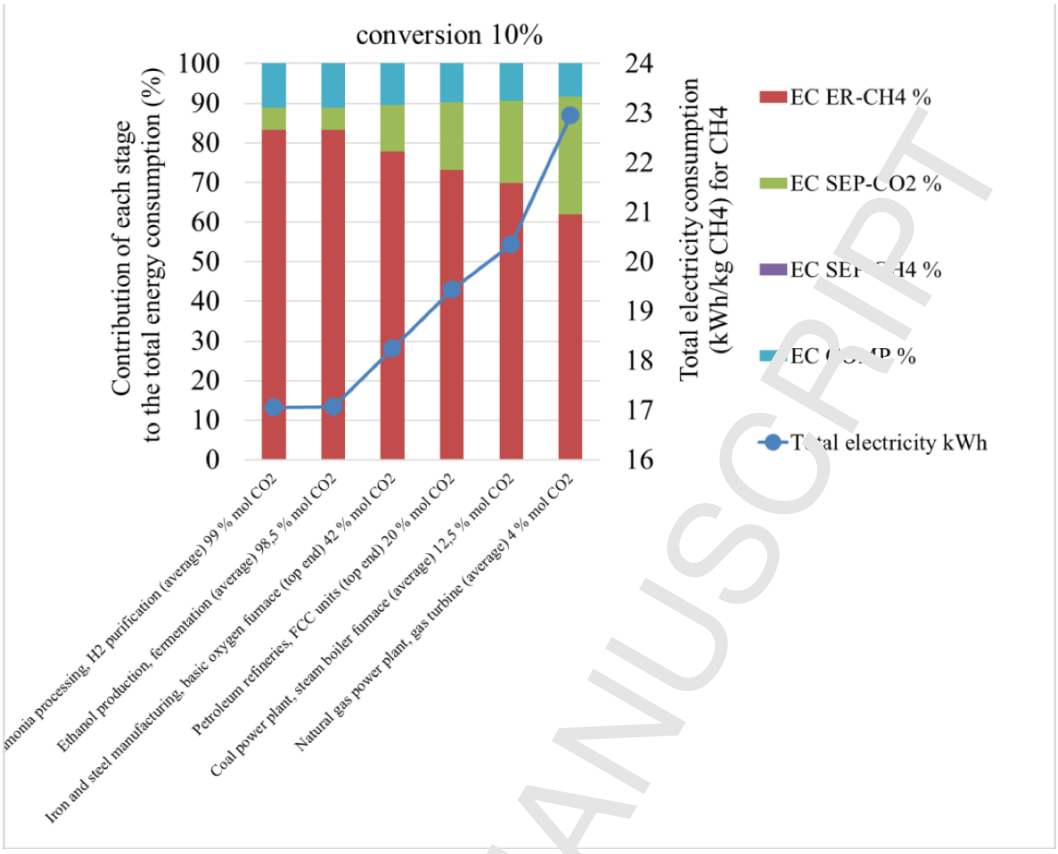

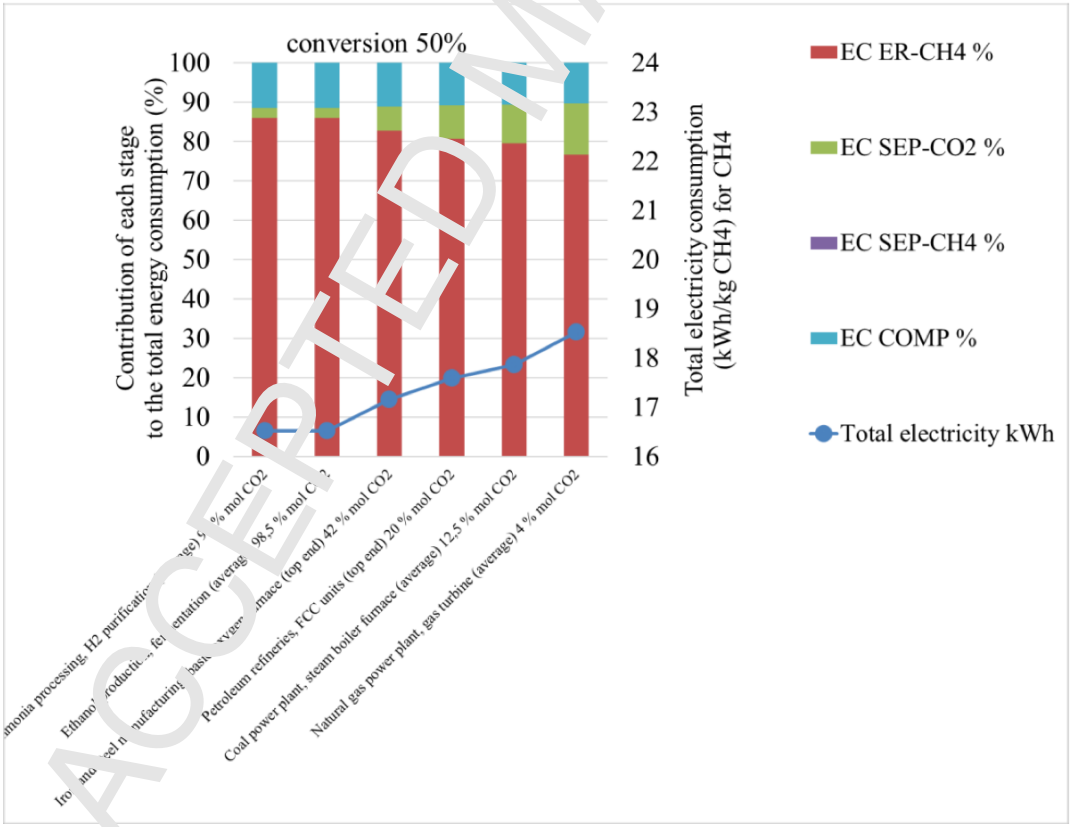

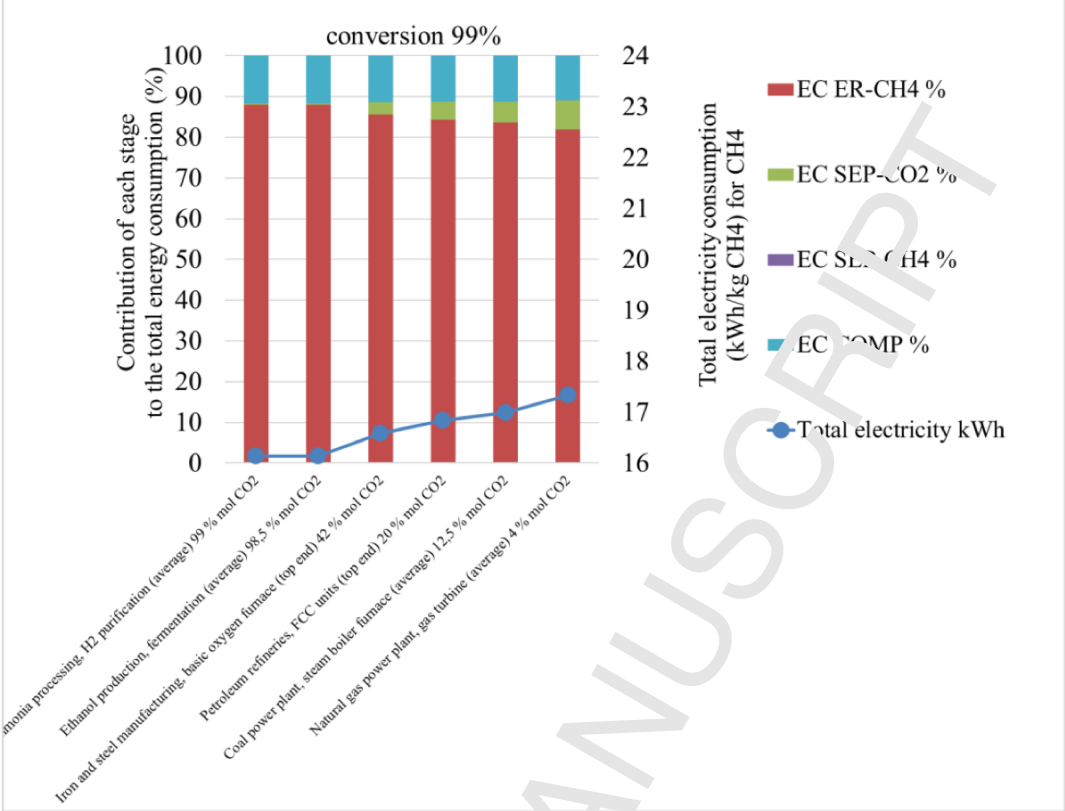

Figure 3. Influence of the upstream CO_2 source: contribution of each stage to the total energy consumption as a function of the selected CO_2 source for a reference ER reactor (0 mV overpotential and a value of 100% for the FE_{CH_4}). a) X_{CO_2} CO_2 conversion 10%, b) X_{CO_2} CO_2 conversion 50%, c) X_{CO_2} CO_2 conversion 99%. The SEC_{ER-CH_4} of the reference ER is 14.2 kWh·kg^{-1}.

3.2 Effect of the faradaic efficiency and the cathode potential (reaction)

From the previous analysis, it is clear that the process benefits from the highest possible CO_2 conversion. Here we have considered an intermediate conversion X_{CO_2} of 50%. A reference ER reactor is used as benchmark for a proper comparison including the most diluted source of CO_2 (4 %) which leads to a molar ratio N_2:CO_2 of 24. Due to experimental results being used the simultaneous effect of the FE_{iR} and the U_C is considered.

Regarding the distribution of products, Table 2 of the SI shows the mass balance for the entire process for the selected references, considering that the basis for the calculation is 1 kg of CH_4. Although relevant quantities of C_2H_4 are produced, it is evident that the main gaseous product of the reduction reaction on a mass basis is CH_4. A key issue is the production of HCOOH in the liquid phase. The production of HCOOH can be as high as 3.42 kg·kg^{-1} of CH_4. This product has an insignificant market share compared to SNG. Consequently, its

production is unnecessary and must be avoided unless a valorisation route is discovered for a particular scenario. With the target of a massive production of CH_4 by this electrochemical PtG route, the valorization of massive amounts of HCOOH seems to be quite difficult. However, current developments are aiming at catholyte-free ER process for HCOOH (Lee et al., 2018), which substantially should increase the product concentration thus reducing the amount of steam needed for separation which is the main drawback for its valorisation (Dominguez-Ramos et al., 2015). Additionally, large amounts of O_2 are produced in the anode, so a way to its valorisation is necessary. Indeed, the process could be potentially connected to the corresponding CO_2 source as in the described example of burning NG. This would led to a process in which O_2 is supplied by the ER plant rather than from an air separation unit, avoiding the separation of the CO_2/N_2 mixture. The greatest variation among used references is found in the production of H_2 and CO. In this work, H_2:CO molar ratios obtained range from 0.1 to 28, making some of them valid for the use as syngas for Fischer-Tropsch processing, while the other must be valorised as H_2. Additional purification must be necessary here. Considering the size, the in-situ valorization of the H_2 or syngas should be discussed. The production of HCOOH should be suppressed as much as possible if valorisation is not possible.

Figure 4 displays the contribution of the different k stages to the EC_{CH_4} taking into account the best performers at lab-scale. Due to the previous discussion regarding HCOOH, the value of EC_{DIST} is not added to the total value of EC_{CH_4}. A maximum value of $88.8 \cdot 10^3$ MJ·kg^{-1} (equivalent to 24.7 kWh·kg^{-1}) would be potentially obtained for EC_{DIST}. The fact that the EC_{ER-CH_4} has a contribution in the range from 82% to 92% means that the ER stage has the highest contribution to the overall process thus all efforts must be directed towards the reduction of the U_C as much as possible. The difference between the energy consumption of the reference ER reactor EC_{REF-CH_4} with a value of 18.5 kWh·kg^{-1} (with a X_{CO_2} of 50%) and the minimum energy specific consumption SEC_{ER-CH_4} with a value of 14.2 kWh·kg^{-1} is the accounting of the EC_{SEP-CO_2} and EC_{COMP}. The ratio of the total electricity consumption EC_{CH_4} related to the total electricity consumption for the reference ER reactor EC_{REF-CH_4} goes from 2.6 to 6.2, which explains the large contribution of EC_{ER-CH_4} to EC_{CH_4}. The EC_{SEP-CO_2} has a small contribution to the overall EC_{CH_4}, ranging from 3.3% to 8.3%. Surprisingly, the EC_{SEP-CH_4} has little effect on EC_{CH_4}, just in the interval from 1.7% to 3.7%. The separation of CO_2 from N_2 from the flue gas of a coal-fired power plant is well-

established at values over the minimum thermodynamic value of 110 kWh·t^{-1} of separated CO_2; current values can be as low as 200 kWh·t^{-1} of separated CO_2, including compression to 150 bar (Boot-Handford et al., 2014). A value of 0.25 kWh·m^{-3} (assumed as m^3 of feed) was reported to deal with the real separation of the unconverted CO_2 by pressure swing adsorption (PSA) as technology (Jouny et al., 2018). In the case of the conditions of the best performer (Manthiram et al., 2014), the equivalent values would be 1,163 kWh·t^{-1} of separated CO_2 (the additional separation of CH_4 is included and a much more diluted CO_2 stream is considered than in coal-fired power plants) and 0.08 kWh·m^{-3}. In the hypothetical case the CO_2 stream would be 12% molar (the remaining 78% as N_2, thus no CH_4 separation), the chosen value of f_{SEP-CO_2} would lead to 290 kWh·t^{-1} of separated CO_2 and 0.06 kWh·m^{-3}. Consequently, the obtained values of EC_{SEP-CO_2} are in the expected order of magnitude. For the separation of CH_4 at 50% wt. from other products, it was reported values up to 1.1 MJ·kg^{-1} of CH_4 in unwanted gas by membrane pressurization and 8.2 MJ·kg^{-1} of CH_4 in CO_2 by PSA (Greenblatt et al., 2018). Again, for the best performer (Manthiram et al., 2014), the equivalent value is close to the reported ranges, thus 12.9 MJ·kg^{-1} of CH_4 (3.59 kWh·kg^{-1} of CH_4) was obtained. This value is lower than the minimum SEC_{ER-CH_4} value of 14.2 kWh·kg^{-1} of CH_4), which points out the fact that the ER process demands considerably more energy than the separation. Electricity is assumed here as the energy vector for the separation of the mixture of gases by PSA or membrane technology. The actual separation of CO_2 using aqueous monoethanolamine (MEA) solutions (30% wt. in MEA) uses industrial heat to deal with the separation. This separation is far away from being trivial due to the difficulties to choose or design efficient solvents which improve the economical indicators of the process (Mota-Martinez et al., 2017). Consequently, it can be confirmed that the selected approach for the product separation provides figures according to previous published studies. It is worthy to mention that the selected approach is not affected by the order of the cascade separation, thus different configurations would potentially lead to similar values of EC_{CH_4}.

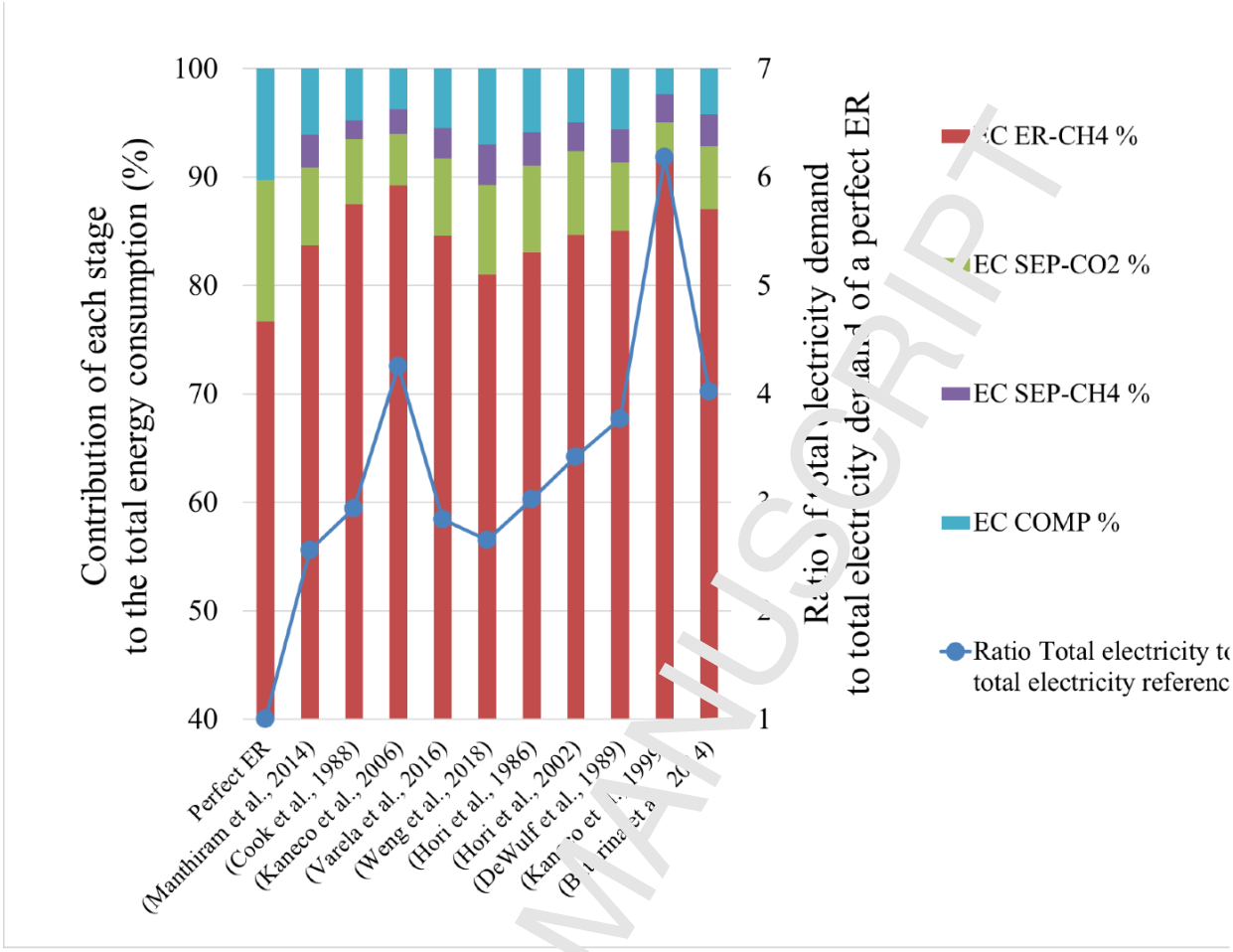

Figure 4. Contribution of each k stage to the total energy consumption EC_{CH_4} for the selected references of top performers. The LC_{REF-CH_4} is 18.5 kWh·kg^{-1}.

3.3 The effect of the carbon footprint in the PV solar powered ER of CO_2 to CH_4

Previous section has displayed the amount of the different i products that can be technically achievable by means of the PV solar powered ER, considering the different k stages. However, it is difficult to claim the possibility to valorise all the products apart from CH_4 and C_2H_4 due to market restrictions. To provide the most possible conservative approach, the carbon footprint associated with just these two predominant products CF_{CH_4} will be considered. This means that the avoided burdens from the other potential avoided products (H_2/CO, O_2, and HCOOH) are not taken into account. The electricity demanded by H_2/CO and O_2 separation and compression will be accounted for even if the two products are not valorised. The same cannot be hold true for HCOOH due to the amount of thermal energy required.

As all the energy requirements are due to the electricity demanded by the process, Figure 5 reports the carbon footprint associated with the production of 1 kg of CH_4 CF_{CH_4} and the

corresponding amounts of all products but HCOOH (as stated in Table 2 of the SI) as a function of the carbon footprint of the PV reference used.

Horizontal thick solid lines represents the carbon footprint associated with the commercial production of the two products (Ecoinvent, 2017). The green solid line is the value for the global average distribution of natural gas at high pressure CF_{Eco-NG} with a value of 0.46 kg·kg^{-1} (Ecoinvent, 2017). The reported $CF_{Eco-C_2H_4}$ is 1.43 kg·kg^{-1} (Ecoinvent, 2017). The top red solid line is the maximum $CF_{Eco-Max}$ value that would be obtained among the chosen case of studies (1.03 kg·kg^{-1}) because of the production of CH_4 (1 kg) and C_2H_4 (0.40 kg). The rationality for the selection of these two values as reference is based on the average production. As the distribution of NG at high pressure reports a global average of CF_{Eco-NG} of 0.46 kg·kg^{-1} (Ecoinvent, 2017), the production of 1 kg of CH_4 by the PV solar powered ER will avoid those emissions. Around 50% of the CF_{Eco-NG} is due to CO_2 and 30% to CH_4. This value as a proxy value for the production of NG seems to be reasonable. The horizontal ocean blue thick line represents the mass ratio CO_2:CH_4 in a perfect combustion, thus highlighting the limit for an overall carbon neutral process (2.75 kg·kg^{-1}).

Vertical dotted lines in Figure 5 represents the CF_{PV} of the different selected sources: current average PV solar (high) CF_{PV-H}, current average PV solar (low) CF_{PV-L}, and future 2050 PV solar CF_{PV-F}, whose values are 58·10^{-3} kg·kWh^{-1}, 14·10^{-3} kg·kWh^{-1} (Hertwich et al., 2015) and 5·10^{-3} kg·kWh^{-1} (Pehl et al., 2017), respectively. The values for current PV solar energy are not simply estimations from theoretical scientific studies. For particular studies of real PV solar facilities, CF_{PV} values as low as 20.2·10^{-3} kg·kWh^{-1} have been already reported (Acciona Energia, 2017). The discussion of the electricity accounted at high, medium or low voltage is out of the scope of this work. The previous range for CF_{PV} fits in the range corresponding to the grid mix of countries with very low CF, in which the mix is dominated hydropower and/or nuclear (Herbert et al., 2016). Therefore, the discussion could be potentially expanded to mixed sources of electricity rather than PV solar technologies. The three remaining lines represents the evolution of the carbon footprint that would be obtained for the maximum energy consumption EC_{Max-CH_4} (78.9 kWh·kg^{-1}), the minimum energy consumption EC_{Min-CH_4} (47.4 kWh·kg^{-1}) and the reference ER energy consumption EC_{REF-CH_4} (63.5 kWh·kg^{-1}).

It is observed that the use of a reference ER process would not accomplish to even the CF_{Eco-NG} of 0.46 kg·kg^{-1} unless the low value CF_{PV-L} of 14·10^{-3} kg·kWh^{-1} is used. As it is evident, the lower the carbon footprint of the PV solar, the better for the PV solar powered

ER process. For the EC_{Max-CH_4} and the EC_{Min-CH_4}, the CF_{PV-L} is not enough to compensate the overall CF_{CH_4}. An ultra-low CF_{PV-F} would put remedy to the situation as a CF_{CH_4} of 0.093 kg·kg^{-1} would be obtained for the consideration of EC_{REF-CH_4}. The valorisation of C_2H_4 can help at offsetting the CF_{CH_4}. Using CF_{PV-L} for the current best performer, it would be possible to even the CF_{CH_4} due to the contribution of C_2H_4 (the horizontal thick red line in Figure 5). Therefore, in order to produce a PtSNG process capable of injecting CH_4 into the NG network using the ER approach discussed in this work, the use of an ultra-low source of electricity is necessary unless the valorization of a parallel product such as C_2H_4 is possible.

Using as reference CF_{PV-H}, the CF_{CH_4} due to the EC_{Max-CH_4} is ~4.5 kg·kg^{-1}. Table 3 reports values obtained in the literature for the PtSNG approach under different hypothesis. As many hypothesis are needed, the benchmark values must be managed carefully. Due to the strong influence of the carbon footprint of the grid mix used and the chosen boundaries (avoided burdens can alter results), the reported range can be wide. However, it can be stated a general range of the CF_{CH_4} from ~1 kg·kg^{-1} to ~10 kg·kg^{-1}. Under the most conservative approach, our value of 4.5 kg·kg^{-1} fits adequately this previous range. We do state that a lower value of the CF_{CH_4} can be pursued under a greener electricity source, without the need of the valorisation of additional products. An ultra-low carbon source would be capable of evening the CF_{Eco-NG}. Indeed, the PV solar powered ER, as an example of PtSNG, should help at the development of additional flexibility of the electricity network backed by the NG network. Let us assume that the energy contained per unit of mass of CH_4, C_2H_4 and H_2 are 50 MJ·kg^{-1}, 47 MJ·kg^{-1} and 120 MJ·kg^{-1} respectively. If so, the overall energy efficiency (ratio energy contained in the products to total electricity input EC_{CH_4}) of the proposed PtSNG would be between 17% and 44%. Consequently, this process would potentially recover a significant amount of the curtailed electricity under high percentage penetration of renewables. Potentially, the EC_{Min-CH_4} could even the emissions of CO_2 from the combustion of pure CH_4 (2.75 kg·kg^{-1}) as represented by the blue ocean horizontal thick line when the carbon footprint of the is CF_{PV-H}.

The technical barriers discussed previously for the PV solar powered ER to CH_4 are being demolished by current developments both in faradaic efficiency, cathode voltage and PV solar efficiency so even if it "*...will require time...*" (Aresta et al., 2013) to reach the proper Technological Readiness Level, it is expected that a more sustainable production of energy is ready on time to meet the global goals related to Climate Change. This work can help at stating the benefits associated with CCU thus promoting its current social acceptance (Perdan

et al., 2017) especially if the comparison versus carbon capture and storage arises (Bruhn et al., 2016).

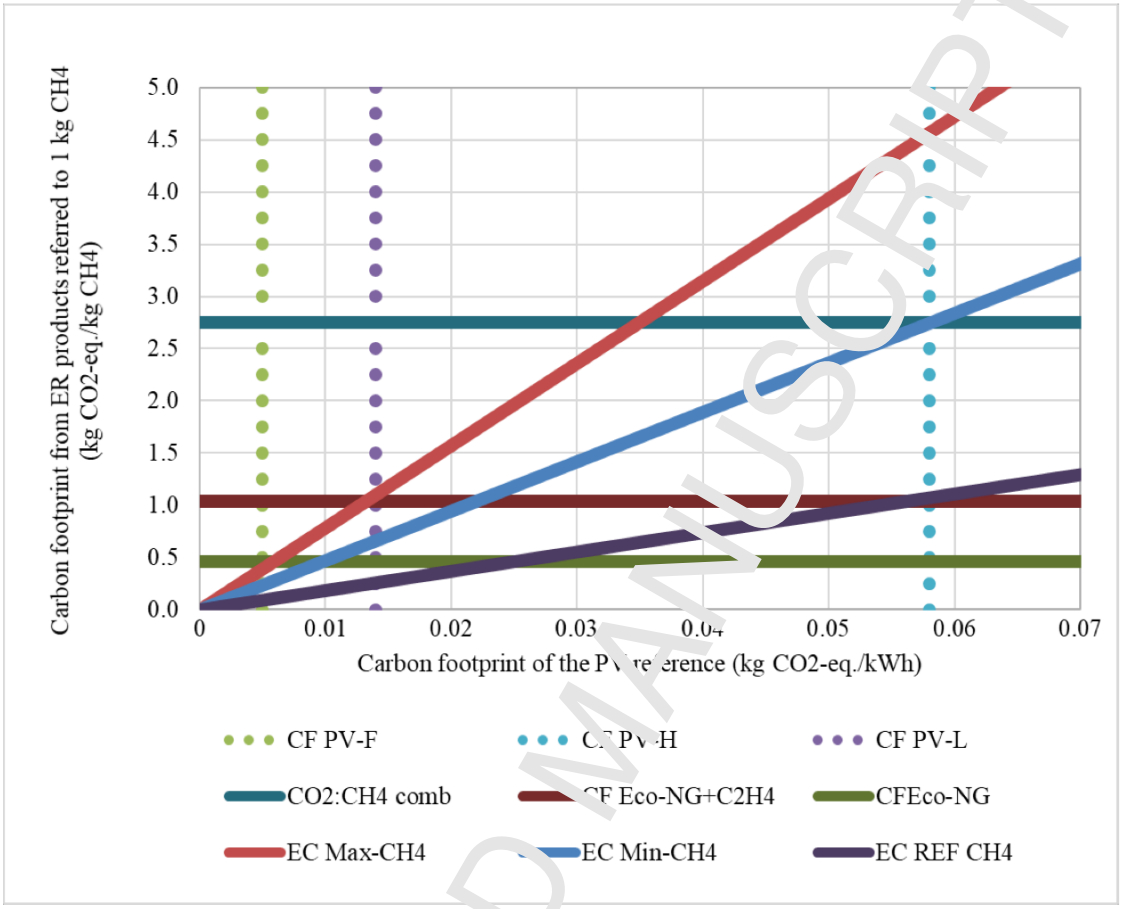

Figure 5. Comparison of the carbon footprint of the performers with the lowest (EC_{Min-CH_4}) and highest (EC_{Max-CH_4}) energy consumption per 1 kg of pure CH_4 and its comparison to the carbon footprint of the products obtained via current global processes.

607 Table 3. The carbon footprint obtained in previous studies regarding PtG (only PtSNG is
608 analysed here). Conversion to adopted values has used a default value of 50.03 $MJ \cdot kg^{-1}$ of
609 CH_4. A generic 2 $MJ \cdot km^{-1}$ was used as tank-to-wheel efficiency for transportation distances
610 of the NG vehicles. The reader is referred to original references for additional details.
611 Methanation is the preferred PtG technology.

612

Reference	CO_2 source	Electricity source	Adopted value ($kg \cdot kg^{-1}$)
(Parra et al., 2017)	Direct Air Capture	Swiss grid mix	3.6
(Collet et al., 2017)	Anaerobic digestion of sewage sludge	French grid mix-EU grid mix	1.25-6.25
(Zhang et al., 2017)	Wood power plant-	PV supply (Swiss)	6.13
	Hard-coal power plant		9.81
(Uusitalo et al., 2017)	-	Wind power	0.25
(Sternberg and Bardow, 2016)	Coal-fired power plant	Variable grid mix	11.1

4. Conclusions

The present study has analysed the Carbon Footprint behind using Photovoltaic (PV) solar energy in order to power an Electrochemical Reduction (ER) of CO_2 to Synthetic Natural Gas (PtSNG). As a novelty, the performance data of the best available cathodes at lab-scale was chosen to feed a model whose output is the mass distribution of products (CH_4, C_2H_4, H_2/CO and HCOOH) and the consumption of energy, mainly as electricity, in each involved stage (reaction, separation of unconverted CO_2, separation of CH_4, and compression to distributable products). The thermal energy for the distillation of HCOOH is not included if no prospects of valorisation does exist.

The influence of the purity of the CO_2 source was analysed for a reference ER reactor producing only CH_4. Even if a conversion of 10% for CO_2 is considered, for the most diluted CO_2 stream at 4% molar, the energy consumption of the ER is by far the main contributor with values over 60%. Higher concentrations and conversions leads to even higher contributions of the ER stage. For currents developments at lab-scale, a diluted source at 4% molar of CO_2 is used (molar ratio N_2:CO_2 is 24) and a conversion of CO_2 is fixed at 50%. In this case, the energy consumption of the ER (not including distillation of HCOOH) is about 2.6 to 6.2 times the one from using the reference ER (18.5 $kWh \cdot kg^{-1}$ of CH_4). Thus, the contribution of the ER is in the range between 81% to 92%. This large contribution is related to the actual cathode overpotentials and faradaic efficiencies, which carries large penalties. To compensate for the energy consumption, low carbon sources must be used to power the process and to obtain a ready-to-inject SNG. The valorisation of C_2H_4 as coproduct can help at the offsetting of the overall carbon footprint so under current developments the use of PV solar energy can even the current carbon footprint of the obtained products versus the equivalent production of NG (average world extraction and distribution) and C_2H_4. Future PV technology will allow to reduce even further the associated carbon footprint.

The proposed PV solar powered ER is a technology to be developed as the actual state-of the-art prevents its utilization due to the low stability of the cathodes, which prevent its industrial use. The great potential, as in PtG technology, relies in the interaction between the electric network and the NG network, providing flexibility in the operation due to the possibility of using curtailed electricity without the need of the intervention of H_2 as intermediate.

5. Acknowledgements

Authors gratefully acknowledge the funding provided by the State Research Agency, Spanish Ministry of Economy and Competitiveness (Spain) through the project CTQ2016-76231-C2-1-R.

6. References

Abanades, J.C., Rubin, E.S., Mazzotti, M., Herzog, H.J., 2017. On the climate change mitigation potential of CO2 conversion to fuels. Energy Environ. Sci. 10, 2491–2499. doi:10.1039/C7EE02819A

Acciona Energia, 2017. Environmental Product Declaration- Electricity generated in photovoltaic power plant El Romero Solar 196 MW.

Agarwal, A.S., Zhai, Y., Hill, D., Sridhar, N., 2011. The electrochemical reduction of carbon dioxide to formate/formic acid: Engineering and economic feasibility. ChemSusChem 4, 1301–1310. doi:10.1002/cssc.201100220

Albo, J., Alvarez-Guerra, M., Castaño, P., Irabien, A., 2015. Towards the electrochemical conversion of carbon dioxide into methanol. Green Chem. 17, 2304–2324. doi:10.1039/C4GC02453B

Albo, J., Beobide, G., Castaño, P., Irabien, A., 2017. Methanol electrosynthesis from CO2 at Cu2O/ZnO prompted by pyridine-based aqueous solutions. J. CO2 Util. 18, 164–172. doi:10.1016/j.jcou.2017.02.003

Alvarez-Guerra, M., Del Castillo, A., Irabien, A., 2014. Continuous electrochemical reduction of carbon dioxide into formate using a tin cathode: Comparison with lead cathode. Chem. Eng. Res. Des. 92, 692–701. doi:10.1016/j.cherd.2013.11.002

Appel, A.M., Bercaw, J.E., Bocarsly, A.B., Dobbek, H., Dubois, D.L., Dupuis, M., Ferry, J.G., Fujita, E., Hille, R., Kenis, P.J.A., Kerfeld, C.A., Morris, R.H., Peden, C.H.F., Portis, A.R., Ragsdale, S.W., Rauchfuss, T.B., Reek, J.N.H., Seefeldt, L.C., Thauer, R.K., Waldrop, G.L., 2013. Frontiers, opportunities, and challenges in biochemical and chemical catalysis of CO2 fixation. Chem. Rev. 113, 6621–6658. doi:10.1021/cr300463y

Aresta, M., Dibenedetto, A., Angelini, A., 2013. The changing paradigm in CO2utilization. J. CO2 Util. 3–4, 65–73. doi:10.1016/j.jcou.2013.08.001

Artz, J., Müller, T.E., Thenert, K., Kleinekorte, J., Meys, R., Sternberg, A., Bardow, A., Leitner, W., 2018. Sustainable Conversion of Carbon Dioxide: An Integrated Review of Catalysis and Life Cycle Assessment. Chem. Rev. 118, 434–504. doi:10.1021/acs.chemrev.7b00435

Aspen Tech, 2018. Aspen Plus. Products Catalogue [WWW Document]. URL https://www.aspentech.com/en/products/engineering/aspen-plus

Bailera, M., Lisbona, P., Romeo, L.M., Espatolero, S., 2017. Power to Gas projects review:

Lab, pilot and demo plants for storing renewable energy and CO2. Renew. Sustain. Energy Rev. 69, 292–312. doi:10.1016/j.rser.2016.11.130

Bains, P., Psarras, P., Wilcox, J., 2017. CO2 capture from the industry sector. Prog. Energy Combust. Sci. 63, 146–172. doi:10.1016/j.pecs.2017.07.001

Baturina, O.A., Lu, Q., Padilla, M.A., Xin, L., Li, W., Serov, A., Artyushkova, K., Atanassov, P., Xu, F., Epshteyn, A., Brintlinger, T., Schuette, M., Collins, G.E., 2014. CO2 electroreduction to hydrocarbons on carbon-supported Cu nanoparticles. ACS Catal. 4, 3682–3695. doi:10.1021/cs500537y

Boot-Handford, M.E., Abanades, J.C., Anthony, E.J., Blunt, M.J., Brandani, S., Mac Dowell, N., Fernández, J.R., Ferrari, M.-C., Gross, R., Hallett, J.P., Haszeldine, R.S., Heptonstall, P., Lyngfelt, A., Makuch, Z., Mangano, E., Porter, R.T.J., Pourkashanian, M., Rochelle, G.T., Shah, N., Yao, J.G., Fennell, P.S., 2014. Carbon capture and storage update. Energy Environ. Sci. 7, 130–189. doi:10.1039/C3EE42350F

Breyer, C., Bogdanov, D., Gulagi, A., Aghahosseini, A., Barbosa, L.S.N.S., Koskinen, O., Barasa, M., Caldera, U., Afanasyeva, S., Child, M., Farfan, J., Vainikka, P., 2017. On the role of solar photovoltaics in global energy transition scenarios. Prog. Photovoltaics Res. Appl. 25, 727–745. doi:10.1002/pip.2885

Bruhn, T., Naims, H., Olfe-Kräutlein, B., 2016. Separating the debate on CO2 utilisation from carbon capture and storage. Environ. Sci. Policy 60, 38–43. doi:10.1016/j.envsci.2016.03.001

Chen, A., Lin, B.-L., 2018. A Simple Framework for Quantifying Electrochemical CO2 Fixation. Joule 2, 1–13. doi:10.1016/j.joule.2018.02.003

Collet, P., Flottes, E., Favre, A., Raynal, L., Pierre, H.H., Capela, S., Peregrina, C., 2017. Techno-economic and Life Cycle Assessment of methane production via biogas upgrading and power to gas technology. Appl. Energy 192, 282–295. doi:10.1016/j.apenergy.2016.08.181

Cook, R.L., 1988. On the Electrochemical Reduction of Carbon Dioxide at In Situ Electrodeposited Copper. J. Electrochem. Soc. 135, 1320. doi:10.1149/1.2095972

Cuéllar-Franca, R.M., Azapagic, A., 2015. Carbon capture, storage and utilisation technologies: A critical analysis and comparison of their life cycle environmental impacts. J. CO2 Util. 9, 82–102. doi:10.1016/j.jcou.2014.12.001

Del Castillo, A., Alvarez-Guerra, M., Solla-Gullón, J., Sáez, A., Montiel, V., Irabien, A., 2017. Sn nanoparticles on gas diffusion electrodes: Synthesis, characterization and use for continuous CO2 electroreduction to formate. J. CO2 Util. 18, 222–228.

718 doi:10.1016/j.jcou.2017.01.021
719 Del Castillo, A., Alvarez-Guerra, M., Solla-Gullón, J., Sáez, A., Montiel, V., Irabien, A.,
720 2015. Electrocatalytic reduction of CO2 to formate using particulate Sn electrodes:
721 Effect of metal loading and particle size. Appl. Energy 157, 165–173.
722 doi:10.1016/j.apenergy.2015.08.012
723 DeWulf, D.W., Jin, T., Bard, A.J., 1989. Electrochemical and Surface Studies of Carbon
724 Dioxide Reduction to Methane and Ethylene at Copper Electrodes in Aqueous Solutions.
725 J. Electrochem. Soc. 136, 1686–1691. doi:10.1149/1.2096993
726 Dimitriou, I., García-Gutiérrez, P., Elder, R.H., Cuéllar-Franca, R.M., Azapagic, A., Allen,
727 R.W.K., 2015. Carbon dioxide utilisation for production of transport fuels: process and
728 economic analysis. Energy Environ. Sci. 8, 1775–1789. doi:10.1039/C4EE04117H
729 Dioxide Materials, 2018. Dioxide Materials Has Developed CO2 Electrolyzers With Record
730 Performance [WWW Document]. CO2 Electrolyzers/Technology. URL
731 https://dioxidematerials.com/technology/co2-electrolysis/
732 Dominguez-Ramos, A., Singh, B., Zhang, X., Hertwich, E.G.G., Irabien, A., 2015. Global
733 warming footprint of the electrochemical reduction of carbon dioxide to formate. J.
734 Clean. Prod. 104, 148–155. doi:10.1016/j.jclepro.2013.11.046
735 Dunn, B., Kamath, H., Tarascon, J.M., 2011. Electrical energy storage for the grid: A battery
736 of choices. Science (80-.). 334, 928–935. doi:10.1126/science.1212741
737 Ecoinvent, 2017. Ecoinvent Database 3.3. Ecoinvent Cent.
738 European Power to Gas Platform, 2018. Power to Gas [WWW Document]. Overview. URL
739 http://www.europeanpowertogas.com/about/power-to-gas
740 Fernández-Dacosta, C., Stoicheva, V., Ramirez, A., 2018. Closing carbon cycles: Evaluating
741 the performance of multi-product CO2utilisation and storage configurations in a
742 refinery. J. CO2 Util. 23, 128–142. doi:10.1016/j.jcou.2017.11.008
743 Finnveden, G., Hauschild, M.Z., Ekvall, T., Guinée, J., Heijungs, R., Hellweg, S., Koehler,
744 A., Pennington, D., Suh, S., 2009. Recent developments in Life Cycle Assessment. J.
745 Environ. Manage. 91, 1–21. doi:10.1016/j.jenvman.2009.06.018
746 Ganesh, I., 2016. Electrochemical conversion of carbon dioxide into renewable fuel
747 chemicals – The role of nanomaterials and the commercialization. Renew. Sustain.
748 Energy Rev. 59, 1269–1297. doi:10.1016/j.rser.2016.01.026
749 Gao, S., Lin, Y., Jiao, X., Sun, Y., Luo, Q., Zhang, W., Li, D., Yang, J., Xie, Y., 2016.
750 Partially oxidized atomic cobalt layers for carbon dioxide electroreduction to liquid fuel.
751 Nature 529, 68–71. doi:10.1038/nature16455

752 Goeppert, A., Czaun, M., Jones, J.-P., Surya Prakash, G.K., Olah, G.A., 2014. Recycling of
753 carbon dioxide to methanol and derived products – closing the loop. Chem. Soc. Rev.
754 43, 7995–8048. doi:10.1039/C4CS00122B
755 Götz, M., Lefebvre, J., Mörs, F., McDaniel Koch, A., Graf, F., Bajohr, S., Reimert, R., Kolb,
756 T., 2016. Renewable Power-to-Gas: A technological and economic review. Renew.
757 Energy 85, 1371–1390. doi:10.1016/j.renene.2015.07.066
758 Greenblatt, J.B., Miller, D.J., Ager, J.W., Houle, F.A., Sharp, I.D., 2018. The Technical and
759 Energetic Challenges of Separating (Photo)Electrochemical Carbon Dioxide Reduction
760 Products. Joule. doi:10.1016/j.joule.2018.01.014
761 Herbert, A.S., Azzaro-Pantel, C., Le Boulch, D., 2016. A typology for world electricity mix:
762 Application for inventories in Consequential LCA (CLCA). Sustain. Prod. Consum. 8,
763 93–107. doi:10.1016/j.spc.2016.09.002
764 Hernández, S., Amin Farkhondehfal, M., Sastre, F., Makkee, M., Saracco, G., Russo, N.,
765 2017. Syngas production from electrochemical reduction of CO2: current status and
766 prospective implementation. Green Chem. 19, 2326–2346. doi:10.1039/C7GC00398F
767 Hertwich, E.G., Aloisi de Larderel, J., Arvesen, A., Bayer, P., Bergesen, J., Bouman, E.,
768 Gibon, T., Heath, G., Peña, C., Purohit, P., Ramirez, A., Suh, S., 2015. UNEP. Green
769 Energy Choices: The benefits, risks, and trade-offs of low-carbon technologies for
770 electricity production. Report of the International Resource Panel.
771 Hori, Y., Kikuchi, K., Murata, A., Suzuki, S., 1986. Production of methane and ethylene in
772 electrochemical reduction of carbon dioxide at copper electrode in aqueous
773 hydrogencarbonate solution. Chem. Lett. 15, 897–898. doi:10.1246/cl.1986.897
774 Hori, Y., Takahashi, I., Koga, O., Hoshi, N., 2002. Selective Formation of C2 Compounds
775 from Electrochemical Reduction of CO2 at a Series of Copper Single Crystal Electrodes.
776 J. Phys. Chem. B 106, 15–17. doi:10.1021/jp013478d
777 House, K.Z., Baclig, A.C., Ranjan, M., van Nierop, E.A., Wilcox, J., Herzog, H.J., 2011.
778 Economic and energetic analysis of capturing CO2 from ambient air. Proc. Natl. Acad.
779 Sci. 108, 20428–20433. doi:10.1073/pnas.1012253108
780 Hussain, J., Jónsson, H., Skulason, E., Jónsson, H., 2018. Calculations of product selectivity
781 in electrochemical CO2 reduction Calculations of product selectivity in electrochemical
782 CO 2 reduction. doi:10.1021/acscatal.7b03308
783 International Energy Agency, 2018. Solar PV. Tracking Clean Energy Progress [WWW
784 Document]. URL http://www.iea.org/tcep/power/renewables/solar/
785 Jhong, H.-R. "Molly," Ma, S., Kenis, P.J., 2013. Electrochemical conversion of CO2 to

786 useful chemicals: current status, remaining challenges, and future opportunities. Curr.
787 Opin. Chem. Eng. 2, 191–199. doi:10.1016/j.coche.2013.03.005
788 Jouny, M., Luc, W.W., Jiao, F., 2018. A General Techno-Economic Analysis of CO2
789 Electrolysis Systems. Ind. Eng. Chem. Res. acs.iecr.7b03514.
790 doi:10.1021/acs.iecr.7b03514
791 Kaneco, S., Iiba, K., Suzuki, S., Ohta, K., Mizuno, T., 1999. Electrochemical Reduction of
792 Carbon Dioxide to Hydrocarbons with High Faradaic Efficiency in LiOH/Methanol. J.
793 Phys. Chem. B 103, 7456–7460. doi:10.1021/jp990021j
794 Kaneco, S., Katsumata, H., Suzuki, T., Ohta, K., 2006. Electrochemical reduction of CO2to
795 methane at the Cu electrode in methanol with sodium supporting salts and its
796 comparison with other alkaline salts. Energy and Fuels 20, 409–414.
797 doi:10.1021/ef050274d
798 Kas, R., Hummadi, K.K., Kortlever, R., De Wit, P., Milbrat, A., Luiten-Olieman, M.W.J.,
799 Benes, N.E., Koper, M.T.M., Mul, G., 2016. Three-dimensional porous hollow fibre
800 copper electrodes for efficient and high-rate electrochemical carbon dioxide reduction.
801 Nat. Commun. 7, 1–7. doi:10.1038/ncomms10748
802 Kauffman, D.R., Thakkar, J., Siva, R., Matranga, C., Ohodnicki, P.R., Zeng, C., Jin, R., 2015.
803 Efficient Electrochemical CO2 Conversion Powered by Renewable Energy. ACS Appl.
804 Mater. Interfaces 7, 15626–15632. doi:10.1021/acsami.5b04393
805 Kenis, P.J.A., Dibenedetto, A., Zhang, T., 2017. Carbon Dioxide Utilization Coming of Age.
806 ChemPhysChem 18, 3091–3093. doi:10.1002/cphc.201701204
807 Khezri, B., Fisher, A.C., Pumera, M., 2017. CO2 reduction: the quest for electrocatalytic
808 materials. J. Mater. Chem. A 5, 8230–8246. doi:10.1039/C6TA09875D
809 Kondratenko, E. V., Mul, G., Baltrusaitis, J., Larrazábal, G.O., Pérez-Ramírez, J., Javier
810 Pérez-Ramírez, J.V K.G.M.J.B.G.O.L., 2013. Status and perspectives of CO2
811 conversion into fuels and chemicals by catalytic, photocatalytic and electrocatalytic
812 processes. Energy Environ. Sci. 6, 3112–3135. doi:10.1039/c3ee41272e
813 Kopljar, D., Wagner, N., Klemm, E., 2016. Transferring Electrochemical CO2 Reduction
814 from Semi-Batch into Continuous Operation Mode Using Gas Diffusion Electrodes.
815 Chem. Eng. Technol. 39, 2042–2050. doi:10.1002/ceat.201600198
816 Lee, C.H., Kanan, M.W., 2015. Controlling H+ vs CO2 Reduction Selectivity on Pb
817 Electrodes. ACS Catal. 5, 465–469. doi:10.1021/cs5017672
818 Lee, J.H.Q., Lauw, S.J.L., Webster, R.D., 2016. The electrochemical reduction of carbon
819 dioxide (CO2) to methanol in the presence of pyridoxine (vitamin B6). Electrochem.

commun. 64, 69–73. doi:10.1016/j.elecom.2016.01.016

Lee, W., Kim, Y.E., Youn, M.H., Jeong, S.K., Park, K.T., 2018. Catholyte-Free Electrocatalytic CO2 Reduction into Formate. Angew. Chemie Int. Ed. 10–15. doi:10.1002/anie.201803501

Li, H., Oloman, C., 2005. The electro-reduction of carbon dioxide in a continuous reactor. J. Appl. Electrochem. 35, 955–965. doi:10.1007/s10800-005-7173-4

Li, X., Anderson, P., Jhong, H.-R.M., Paster, M., Stubbins, J.F., Kenis, P.J.A., 2016. Greenhouse Gas Emissions, Energy Efficiency, and Cost of Synthetic Fuel Production Using Electrochemical CO2 Conversion and the Fischer-Tropsch Process. Energy and Fuels 30, 5980–5989. doi:10.1021/acs.energyfuels.6b00665

Liu, C., Li, F., Ma, L.-P., Cheng, H.-M., 2010. Advanced Materials for Energy Storage. Adv. Mater. 22, E28–E62. doi:10.1002/adma.200903328

Majumdar, A., Deutch, J.M., 2018. Research Opportunities for CO2 Utilization and Negative Emissions at the Gigatonne-Scale. Joule (in press), 805–809. doi:10.1016/j.joule.2018.04.018

Manthiram, K., Beberwyck, B.J., Alivisatos, A.P., 2014. Enhanced electrochemical methanation of carbon dioxide with a dispersible nanoscale copper catalyst. J. Am. Chem. Soc. 136, 13319–13325. doi:10.1021/ja5065284

Martin, A.J., Larrazabal, G.O., Perez-Ramirez, J., 2015. Towards sustainable fuels and chemicals through the electrochemical reduction of CO2: lessons from water electrolysis. Green Chem. 17, 5114–5130. doi:10.1039/C5GC01893E

Mazza, A., Bompard, E., Chicco, G., 2018. Applications of Power to Gas technologies in Emerging Electrical Systems. Renew. Sustain. Energy Rev. 92, 1–42. doi:10.1016/j.rser.2018.04.072

Merino-Garcia, I., Albo, J., Irabien, A., 2018. Tailoring gas-phase CO2 electroreduction selectivity to hydrocarbons at Cu nanoparticles. Nanotechnology 29. doi:10.1088/1361-6528/aa9943

Merino-Garcia, I., Albo, J., Irabien, A., 2017. Productivity and Selectivity of Gas-Phase CO2 Electroreduction to Methane at Copper Nanoparticle-Based Electrodes. Energy Technol. 5, 922–928. doi:10.1002/ente.201600616

Merino-Garcia, I., Alvarez-Guerra, E., Albo, J., Irabien, A., 2016. Electrochemical membrane reactors for the utilisation of carbon dioxide. Chem. Eng. J. 305, 104–120. doi:10.1016/j.cej.2016.05.032

Min, X., Kanan, M.W., 2015. Pd-Catalyzed Electrohydrogenation of Carbon Dioxide to

Formate: High Mass Activity at Low Overpotential and Identification of the Deactivation Pathway. J. Am. Chem. Soc. 137, 4701–4708. doi:10.1021/ja511890h

Mota-Martinez, M.T., Hallett, J.P., Mac Dowell, N., 2017. Solvent selection and design for CO2 capture – how we might have been missing the point. Sustain. Energy Fuels 1, 2078–2090. doi:10.1039/C7SE00404D

Natsui, K., Iwakawa, H., Ikemiya, N., Nakata, K., Einaga, Y., 2018. Stable and Highly Efficient Electrochemical Production of Formic Acid from Carbon Dioxide Using Diamond Electrodes. Angew. Chemie - Int. Ed. 57, 2639–2643. doi:10.1002/anie.201712271

Olah, G.A., Goeppert, A., Prakash, G.K.S., 2009. Beyond Oil and Gas: The Methanol Economy: Second Edition. Beyond Oil Gas Methanol Econ Second Ed. 1–334. doi:10.1002/9783527627806

Oloman, C., Li, H., 2008. Electrochemical processing of carbon dioxide. ChemSusChem 1, 385–391. doi:10.1002/cssc.200800015

Pander III, J.E., Ren, D., Yeo, B.S., 2017. Practices for the collection and reporting of electrocatalytic performance and mechanistic information for the CO2 reduction reaction. Catal. Sci. Technol. doi:10.1039/C7CY01785E

Parra, D., Zhang, X., Bauer, C., Patel, M.K., 2017. An integrated techno-economic and life cycle environmental assessment of power-to-gas systems. Appl. Energy 193, 440–454. doi:10.1016/j.apenergy.2017.02.063

Pehl, M., Arvesen, A., Humpenöder, F., Popp, A., Hertwich, E.G., Luderer, G., 2017. Understanding future emissions from low-carbon power systems by integration of life-cycle assessment and integrated energy modelling. Nat. Energy 2, 939–945. doi:10.1038/s41560-017-0032-9

Perdan, S., Jones, C.R., Azapagic, A., 2017. Public awareness and acceptance of carbon capture and utilisation in the UK. Sustain. Prod. Consum. 10, 74–84. doi:10.1016/j.spc.2017.01.001

Qiao, J., Liu, Y., Hong, F., Zhang, J., 2014. A review of catalysts for the electroreduction of carbon dioxide to produce low-carbon fuels. Chem. Soc. Rev. 43, 631–675. doi:10.1039/c3cs60323g

Reiter, G., Lindorfer, J., 2015. Global warming potential of hydrogen and methane production from renewable electricity via power-to-gas technology. Int. J. Life Cycle Assess. 20, 477–489. doi:10.1007/s11367-015-0848-0

Rosen, B.A., Salehi-Khojin, A., Thorson, M.R., Zhu, W., Whipple, D.T., Kenis, P.J., Masel,

R.I., 2011. Ionic liquid-mediated selective conversion of CO(2) to CO at low overpotentials. Science (80-.). 334, 643–644. doi:10.1126/science.1209786

Ross, M.B., Dinh, C.T., Li, Y., Kim, D., De Luna, P., Sargent, E.H., Yang, P., 2017. Tunable Cu Enrichment Enables Designer Syngas Electrosynthesis from CO2. J. Am. Chem. Soc. 139, 9359–9363. doi:10.1021/jacs.7b04892

Schiebahn, S., Grube, T., Robinius, M., Tietze, V., Kumar, B., Stolten, D., 2015. Power to gas: Technological overview, systems analysis and economic assessment for a case study in Germany. Int. J. Hydrogen Energy 40, 4285–4294 doi:10.1016/j.ijhydene.2015.01.123

Schiffer, Z.J., Manthiram, K., 2017. Electrification and Decarbonization of the Chemical Industry. Joule 1, 10–14. doi:10.1016/j.joule.2017.07.008

Scialdone, O., Galia, A., Nero, G. Lo, Proietto, F., Sabatino, A., Schiavo, B., 2016. Electrochemical reduction of carbon dioxide to formic acid at a tin cathode in divided and undivided cells: Effect of carbon dioxide pressure and other operating parameters. Electrochim. Acta 199, 332–341. doi:10.1016/j.electacta.2016.02.079

Sebastián, D., Palella, A., Baglio, V., Spadaro, L., Siracusano, S., Negro, P., Niccoli, F., Aricò, A.S., 2017. CO2 reduction to alcohols in a polymer electrolyte membrane co-electrolysis cell operating at low potentials. Electrochim. Acta 241, 28–40. doi:10.1016/j.electacta.2017.04.119

Singla, R., Chowdhury, K., 2017. Mitigating an increase of specific power consumption in a cryogenic air separation unit at reduced oxygen production, in: IOP Conference Series: Materials Science and Engineering. doi:10.1088/1757-899X/171/1/012016

Spurgeon, J., Kumar, B., 2018. A comparative technoeconomic analysis of pathways for commercial electrochemical CO2 reduction to liquid products. Energy Environ. Sci. 0–18. doi:10.1039/C8EE00097B

Sternberg, A., Bardow, A., 2016. Life Cycle Assessment of Power-to-Gas: Syngas vs Methane. ACS Sustain. Chem. Eng. 4, 4156–4165. doi:10.1021/acssuschemeng.6b00644

United Nations, 2015. Transforming our world: the 2030 Agenda for Sustainable Development. Gen. Assem. Seventieth Sess. 16301, 1–35. doi:10.1007/s13398-014-0173-7.2

Uusitalo, V., Väisänen, S., Inkeri, E., Soukka, R., 2017. Potential for greenhouse gas emission reductions using surplus electricity in hydrogen, methane and methanol production via electrolysis. Energy Convers. Manag. 134, 125–134.

doi:10.1016/j.enconman.2016.12.031

Varela, A.S., Kroschel, M., Reier, T., Strasser, P., 2016. Controlling the selectivity of CO2 electroreduction on copper: The effect of the electrolyte concentration and the importance of the local pH. Catal. Today 260, 8–13. doi:10.1016/j.cattod.2015.06.009

Verma, S., Kim, B., Jhong, H.-R.M., Ma, S., Kenis, P.J.A., 2016. A Gross-Margin Model for Defining Technoeconomic Benchmarks in the Electroreduction of CO2. ChemSusChem 9, 1972–1979. doi:10.1002/cssc.201600394

von der Assen, N., Jung, J., Bardow, A., 2013. Life-cycle assessment of carbon dioxide capture and utilization: avoiding the pitfalls. Energy Environ. Sci. 6, 2721. doi:10.1039/c3ee41151f

Weng, Z., Wu, Y., Wang, M., Jiang, J., Yang, K., Huo, S., Wang, X.F., Ma, Q., Brudvig, G.W., Batista, V.S., Liang, Y., Feng, Z., Wang, H., 2018. Active sites of copper-complex catalytic materials for electrochemical carbon dioxide reduction. Nat. Commun. 9. doi:10.1038/s41467-018-02819-3

Whipple, D.T., Kenis, P.J.A., 2010. Prospects of CO2 utilization via direct heterogeneous electrochemical reduction. J. Phys. Chem. Lett. 1, 3451–3458. doi:10.1021/jz1012627

Yang, H., Kaczur, J.J., Sajjad, S.D., Masel, R.I., 2017. Electrochemical conversion of CO 2 to formic acid utilizing Sustainion^{TM} membranes. J. CO2 Util. 20, 208–217. doi:10.1016/j.jcou.2017.04.011

Yang, Z., Zhang, J., Kintner-meyer, M.C.W., Lu, X., Choi, D., Lemmon, J.P., Liu, J., 2011. Electrochemical energy storage for green grid.pdf. Chem. Rev. 111, 3577–613. doi:10.1021/cr100290v

Zhang, S., Kang, P., Meyer, T.J., 2014. Nanostructured tin catalysts for selective electrochemical reduction of carbon dioxide to formate. J. Am. Chem. Soc. 136, 1734–1737. doi:10.1021/ja411823885

Zhang, W., Hu, Y., Ma, L., Zhu, G., Wang, Y., Xue, X., Chen, R., Yang, S., Jin, Z., 2018. Progress and Perspective of Electrocatalytic CO2 Reduction for Renewable Carbonaceous Fuels and Chemicals. Adv. Sci. 5. doi:10.1002/advs.201700275

Zhang, X., Bauer, C., Mutel, C.L., Volkart, K., 2017. Life Cycle Assessment of Power-to-Gas: Approaches, system variations and their environmental implications. Appl. Energy 190, 326–338. doi:10.1016/j.apenergy.2016.12.098

Zhang, Y., Ji, X., Lu, X., 2014. Energy consumption analysis for CO2 separation from gas mixtures. Appl. Energy 130, 237–243. doi:10.1016/j.apenergy.2014.05.057

Zhao, S., Guo, S., Zhu, C., Gao, J., Li, H., Huang, H., Liu, Y., Kang, Z., 2017. Achieving

electroreduction of CO2 to CH3OH with high selectivity using a pyrite–nickel sulfide nanocomposite. RSC Adv. 7, 1376–1381. doi:10.1039/C6RA26868D

Zhu, Q., Ma, J., Kang, X., Sun, X., Liu, H., Hu, J., Liu, Z., Han, B., 2016. Efficient Reduction of CO2 into Formic Acid on a Lead or Tin Electrode using an Ionic Liquid Catholyte Mixture. Angew. Chemie - Int. Ed. 55, 9012–9016. doi:10.1002/anie.201601974

990

991

992 ## Highlights

993 The carbon footprint (CF) of a PV solar powered electro-reduction for CH_4 was analysed

994 All relevant stages as reaction, separation of CO_2 and CH_4 and compression are included

995 Between 2.6 and 6.2 times is the current electricity consumption compared to reference

996 conditions

997 The main contribution in CF terms is the reaction stage

998 The CF of best performer can even the CF of the existing process for CH_4

999